energies

Review

Vacuum Processability of Self-Assembled Monolayers and Their Chemical Interaction with Perovskite Interfaces

Hyeji Han [1,†], Siwon Yun [1,†], Zobia Irshad [1], Wonjong Lee [1], Min Kim [2,*], Jongchul Lim [1,*] and Jinseck Kim [3,*]

[1] Graduate School of Energy Science & Technology, Chungnam National University, Daejeon 34134, Republic of Korea; gpwl0358@gmail.com (H.H.); wlq247@cnu.ac.kr (S.Y.); chem.zobia@gmail.com (Z.I.); wjong0227@gmail.com (W.L.)
[2] Department of Chemical Engineering, Center for Innovative Chemical Processes, Institute of Engineering, University of Seoul, 163 Seoulsiripdaero, Dongdaemun-gu, Seoul 02504, Republic of Korea
[3] Department of Polymer-Nano Science and Technology, Jeonbuk National University, Jeonju 54896, Republic of Korea
* Correspondence: min.kim@uos.ac.kr (M.K.); jclim@cnu.ac.kr (J.L.); jskim422@jbnu.ac.kr (J.K.)
† These authors contributed equally to this work.

Abstract: Self-assembled monolayers (SAMs) have gained significant attention as an interfacial engineering strategy for perovskite solar cells (PSCs) due to their efficient charge transport ability and work function tunability. While solution-based methods such as dip-coating and spin-coating are widely used for SAM deposition, challenges such as non-uniform coverage, solvent contamination, and limited control over molecular orientation hinder their scalability and reproducibility. In contrast, vacuum deposition techniques, including thermal evaporation, overcome these limitations by enabling the formation of highly uniform materials with precise control over thickness and molecular arrangement. Importantly, the chemical interactions between SAM materials and perovskite layers, including coordination bonding with Pb^{2+} ions, play an important role in passivating surface defects, modulating energy levels, and promoting uniform perovskite crystallization. These interactions not only enhance wettability but also improve the overall quality and stability of perovskite films. This review highlights the advantages of vacuum-deposited SAMs, promoting strong chemical interactions with perovskite layers and improving interfacial properties critical for scalable applications.

Keywords: perovskite; self-assembled monolayer; evaporation; interface properties; chemical interaction

check for updates

Academic Editor: Jürgen Heinz Werner

Received: 16 February 2025
Revised: 29 March 2025
Accepted: 31 March 2025
Published: 2 April 2025

Citation: Han, H.; Yun, S.; Irshad, Z.; Lee, W.; Kim, M.; Lim, J.; Kim, J. Vacuum Processability of Self-Assembled Monolayers and Their Chemical Interaction with Perovskite Interfaces. *Energies* **2025**, *18*, 1782. https://doi.org/10.3390/en18071782

Copyright: © 2025 by the authors. Licensee MDPI, Basel, Switzerland. This article is an open access article distributed under the terms and conditions of the Creative Commons Attribution (CC BY) license (https://creativecommons.org/licenses/by/4.0/).

1. Introduction

Perovskite solar cells (PSCs) have drawn widespread interest for next-generation photovoltaic devices due to their high-power conversion efficiencies (PCEs) and cost-effective fabrication processes [1–5]. Despite these advantages, several challenges remain in enhancing their performance and long-term stability, particularly with respect to charge transport efficiency [6–10]. Among the strategies employed to address these issues, incorporating a self-assembled monolayer (SAM) has been shown to effectively enhance the interfacial charge transport properties, leading to notable improvements in PSC performance [11–14]. The application of SAMs, especially at the interfaces between the transparent metal oxide electrode and perovskite layer, plays a crucial role in perovskite solar cells [15–21].

SAMs act as molecular bridges that modify the interfacial properties of charge transport interfaces [22–26]. This modification improves charge extraction, minimizes non-radiative

recombination losses, and ultimately enhances the power conversion efficiency (PCE) of PSCs [27–29]. Notably, carbazole-based SAMs and phosphonic acid functional group-based SAMs have gained significant attention due to their ability to form strong chemisorption with metal oxide and capable charge extraction from the perovskite layer [30–33].

This review aims to systematically examine the chemical interaction with the SAMs layer at the perovskite interfaces. SAMs are typically composed of molecules with a functional terminal group and an anchoring group, which can form a chemical interaction with the perovskite surface [34–36]. These interactions play a vital role in the passivation of surface defects, consequently reducing trap states and enhancing carrier lifetimes [37]. Additionally, SAMs can modulate surface energy, promoting uniform perovskite crystal growth and improving film morphology [38,39]. However, a comprehensive review on this topic has not yet been conducted.

From other perspectives, the deposition of SAMs via vacuum thermal deposition processes offers distinct advantages for precisely controlling monolayer formation. Compared to solution-based methods, vacuum deposition enables the fabrication of highly uniform and well-ordered SAMs with minimal contamination, which is critical for ensuring consistent interfacial properties in perovskite devices [40,41]. This approach also enables better control over the thickness and orientation of the SAMs, which are essential for effective charge transport optimization [42]. Furthermore, vacuum deposition processes are compatible with fabrication workflows involving vapor-phase deposition techniques, reducing potential cross-contamination and enhancing process continuity [43]. These benefits make vacuum-deposited SAMs particularly suitable for advanced perovskite-based optoelectronic applications. Ultimately, the purpose of this review is to explore the potential of SAMs in perovskite solar cells fabricated through vacuum deposition processes to maximize the utility of SAM by investigating the effects of chemical interactions between SAMs and perovskite materials.

2. Background

2.1. Structural Components of SAM

SAMs comprise three main structural components: a terminal group designed to tailor surface properties and interactions with the perovskite, a linker group that regulates the interfacial characteristics of the monolayer, and an anchoring group that facilitates chemical attachment to the substrate surface (Figure 1) [44,45]. The terminal group typically comprises arylamine derivatives with hole-selective transport properties, including triphenylamine, carbazole, and phenothiazine [46,47]. Due to the hydrophobic nature of these molecular backbones, the contact characteristics with the perovskite can vary significantly depending on functional groups, which can be introduced by organic synthesis [48–50]. This functionalization allows for the modulation of the surface energy, which enhances the quality of the subsequently deposited perovskite film, with better charge extraction and suppression of charge recombination at the perovskite interface [51,52].

The linker group is the molecular backbone connecting the anchoring group and the terminal group, controlling the molecular structure through van der Waals interactions [55]. Two main types of molecules are typically used: non-conjugated alkyl chains and conjugated aromatic groups, each exhibiting distinct charge transport characteristics [56,57]. These linker groups are crucial in determining the molecular alignment during self-assembly. Depending on the length of the alkyl chain or the structure of the aromatic groups, they can influence the dipole moment and tunneling effects at the interface [58–60].

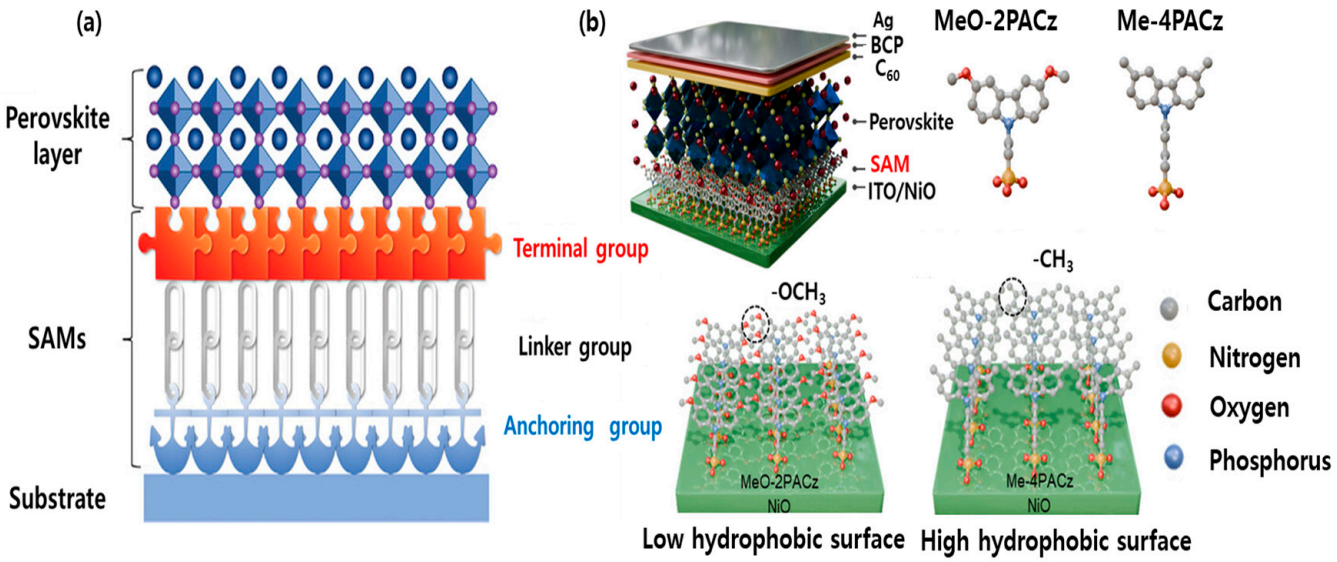


Figure 1. (**a**) The composition and structure of SAM material in perovskite solar cells. Reproduced with permission from ref. [53], copyright 2025 Wiley. (**b**) Schematic of the p-i-n structure PSCs, including the molecular structures of carbazole-based MeO-2PACz and Me-4PACz. Reproduced with permission from ref. [54], copyright 2024 Wiley.

The anchoring group interacts with metal oxides and binds to the metal oxide electrode surface through the chemical adsorption process [61,62]. They interact with hydroxyl groups on the surface of metal oxides, forming mono-, bi-, or tridentate bonds via a condensation reaction between the oxygen atoms of the anchoring group and the metal oxide surface [63,64]. In the case of tridentate bonding, hetero-condensation occurs, with hydrogen atoms migrating to the surface hydroxyl groups, leading to the formation of oxygen vacancies and further bonding interactions. As a result, various binding configurations exist between the SAM and the substrate [65].

2.2. Binding Modes of SAM

The formation of SAM layers involves both chemical adsorption and physical adsorption mechanisms [66]. Chemical adsorption occurs through the formation of covalent bonds between the functional anchoring groups of SAMs and the metal oxide electrode surface, ensuring strong and stable attachment compared to physical interactions (Figure 2) [67]. Concurrently, physical adsorption, driven by weak interactions such as van der Waals forces or electrostatic interactions, is randomly covered on the metal oxide surface [68]. These dual adsorption processes collectively result in the self-assembly of a monolayer, which is essential for achieving desirable interfacial properties in various applications [69–71]. In solution-based processes, SAMs generally have sufficient time and energy to interact with the electrode surface, enabling strong chemical adsorption through mono-, bi-, or tridentate bonding between anchoring groups and metal oxides. Additionally, physically adsorbed SAMs can form overlayers when non-anchored molecules remain on the substrate surface [72]. On the other hand, SAMs with a high degree of order can spontaneously self-assemble during vacuum deposition [73,74].

The bonding modes of SAM materials vary depending on the chemical properties of the anchoring group and the hydroxyl (-OH) group density on the metal oxide surface. Phosphonic acid ($-PO(OH)_2$) is one of the most commonly used anchoring groups, forming strong chemical bonds with metal oxide surfaces and creating monodentate, bidentate, or tridentate bonds [63]. The phosphoryl oxygen of phosphonic acid is directed toward the free acid binding section, increasing the P atom's electrophilicity. This structural

arrangement facilitates the formation of high-energy phosphorus-oxygen-metal oxide bonds through condensation reactions between neighboring hydroxyl groups and surface hydroxyl groups [75–77]. Typically, metal oxide surfaces with extensive hydroxyl groups, such as SnO_2, TiO_2, and indium tin oxide (ITO), favor bidentate or tridentate bonding, providing strong bonding strength and chemical stability [78–81]. In the case of tridentate bonding, three oxygen atoms of phosphonic acid simultaneously bond with hydroxyl groups on the metal oxide surface, improving charge transfer characteristics at the interface and significantly enhancing structural stability [82–85].

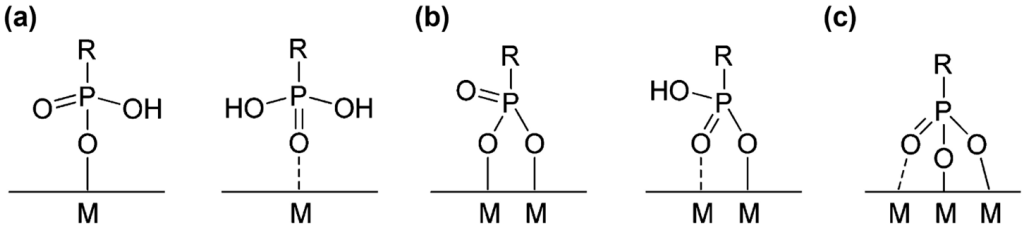


Figure 2. Schematic representation of potential chemisorption between phosphonic acid SAMs and metal oxide substrate, where M = metal oxide. (**a**) Monodentate, (**b**) bidentate, and (**c**) tridentate binding modes. Reproduced with permission from ref. [63], copyright 2008 American Chemical Society.

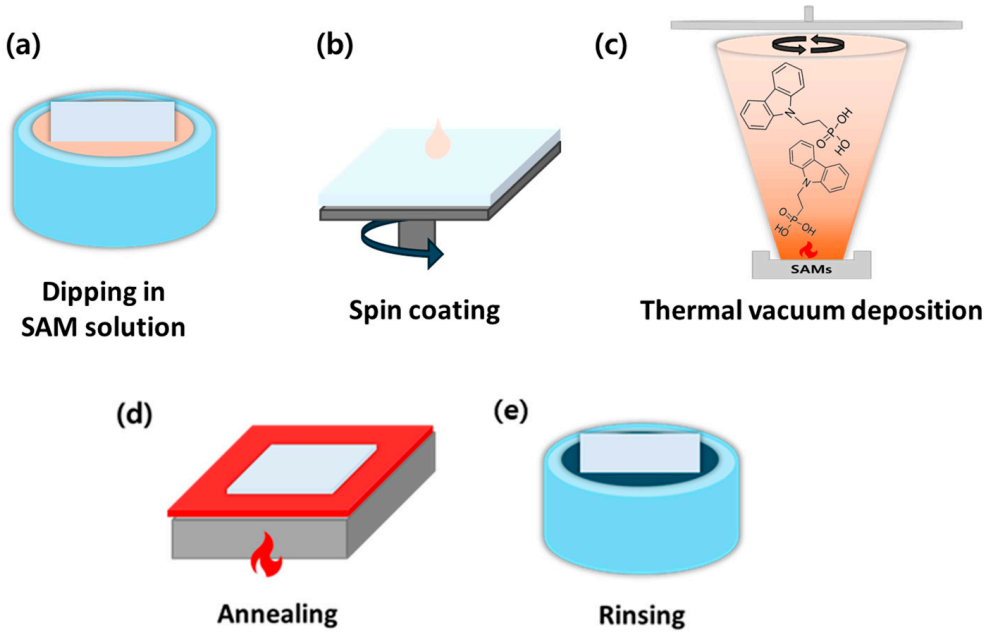
2.3. Processing of SAMs

The properties and quality of the monolayer formed by SAMs highly depend on the specific variables (Figure 3). SAM structure, deposition method, and processing time can potentially affect the formation of chemical bonds or physical adsorption at the substrate interface [86]. Additionally, the nature of the electrode, including its functional groups and chemical composition, plays a critical role in determining the extent of adsorption and molecular organization [87–89]. Variations in these factors can result in significant differences in interfacial properties, such as defect passivation efficiency and surface energy modulation. These disparities ultimately affect the performance, stability, and reproducibility of devices relying on SAM-modified interfaces, highlighting the importance of optimizing the fabrication process to achieve the desired monolayer characteristics [86].

SAM processes are primarily categorized as vapor-phase and liquid-phase deposition techniques. Vapor-phase deposition involves exposing the substrate to a vaporized SAM atmosphere, with post-process thermal annealing employed to enhance the chemical interaction and rapid adsorption of SAM molecules onto the substrate [90]. A notable advantage of this method is to achieve the formation of uniform layers without rinsing. This eliminates additional processing steps and minimizes the risk of disrupting the molecular assembly, thereby ensuring a uniform layer. This process enhances precision and reproducibility by reducing potential contamination and simplifying the deposition process [91].

In contrast, liquid-phase deposition can be further classified into immersion and spin-coating methods. The immersion method, or dip-coating, involves submerging the substrate into a SAM solution, allowing uniform and controlled deposition by a strong chemisorption mechanism [92]. Precise control of SAM solution concentration and immersion time is critical for achieving uniform SAM formation. Low concentrations necessitate longer immersion times, while high concentrations can induce aggregation between SAM molecules, disrupting molecular arrangement and reducing surface properties [88,93]. Thus, optimizing solution concentration and immersion time is essential for producing highly ordered SAMs. The spin-coating method, on the other hand, enables rapid and uniform SAM deposition by regulating the deposition speed of the SAM solution onto the substrate, followed by thermal treatment to remove residual solvent [40,94,95]. Post-annealing treatment further strengthens SAM–substrate bonding, enhancing chemical adsorption. The optimization of an appropriate annealing temperature is crucial

for achieving ordered molecular assembly and controlling the SAM deposition rate and packing density [15,96].



Processing method	Critical parameters
Dipping in SAM solution	Soaking time
Spin coating	Spin rpm coating time
Thermal vacuum deposition	Deposition rate
Annealing	Temperature
Rinsing	Rinsing solvent

Figure 3. Schematic illustration of processing methods and critical parameters of SAMs by (**a**) dipping in SAM solution, (**b**) spin coating, and (**c**) thermal vacuum deposition. Post-treatment process: (**d**) annealing and (**e**) rinsing.

3. Promising for Vacuum Deposition of SAM

The solution processing technique, including dip-coating, spin-coating, and spray-coating, is widely used for SAM deposition [74]. However, solution-based methods face challenges, including inconsistent layer uniformity, potential solvent contamination, and difficulty in controlling the molecular orientation and packing density, which can negatively impact the quality and reproducibility of the SAM layers [58,97]. To address these limitations, vacuum deposition techniques such as thermal evaporation provide a superior alternative. Thermal evaporation is the earliest developed and most widely adopted film-coating technology [98,99]. It is a physical–chemical process by which the raw materials are heated, vaporized, and then deposited onto the substrates under high-vacuum conditions. The maturity and reliability of thermal evaporation make it a competitive route for large-area and scale-up industry fabrication [100–102]. Additionally, thermal evaporation offers distinct advantages for perovskite preparation: it is a solvent-free method that is ideal for inorganic perovskites, enabling precise control over film thickness and uniformity

and providing a high vacuum environment suitable for the fabrication of oxygen-sensitive or metastable perovskites [103,104]. Additionally, the sublimation process during thermal evaporation ensures high purity by reducing impurities and trap density, while its reproducibility addresses challenges such as rapid reaction and crystallization rates seen in solution-based methods [105]. Most importantly, the thermal evaporation of SAM is suitable as a preceding process for vacuum-processed perovskite deposition [106,107].

Building on these advantages, recent advances in vacuum-deposited SAMs have demonstrated significant improvements in PSC performance, highlighting the potential of this approach. In 2023, Farag et al. first investigated the vacuum deposition 2PACz and achieved a PCE of 19.5% [106]. Then, Kore et al. incorporated thermal evaporated 2PACz and Me-4PACz in tandem devices and obtained PCEs of 28.6% and 28.0%, respectively [108]. In addition, Qi et al. compared spin-coating to the thermal evaporation method for 2PACz and achieved a PCE of 19.72% with the latter method [109]. Jen et al. introduced a highly crystalline self-assembled multilayer (SAMUL), and a PCE of 23.50% was achieved by adopting the thermal evaporation method [110]. In 2025, Diercks et al. introduced the sequential evaporation method by using MeO-2PACz; they obtained a PCE of 17.2% [111].

Recent studies have demonstrated the effectiveness and highlighted the advantages of vacuum deposition techniques for the deposition of SAM layers. For instance, Farag et al. reported the first application of vacuum-deposited SAM hole-transport layers in inverted perovskite solar cells (p–i–n architecture). By employing widely used SAMs such as [2-(9H-Carbazol-9-yl)ethyl]phosphonic acid (2PACz), [2-(3,6-Dimethoxy-9H-carbazol-9-yl)ethyl]phosphonic acid (MeO-2PACz), and [4-(3,6-Dimethyl-9H-carbazol-9-yl)butyl]phosphonic acid (Me-4PACz), the study demonstrated that vacuum deposition preserves or even improves interfacial properties, including wettability and energy level alignment compared with solution-processed 2PACz (Figure 4a). In addition, evaporated SAMs exhibit enhanced interface qualities, leading to minimal non-radiative recombination and improved stability. Furthermore, they demonstrated that the evaporated SAMs formed a covalent bond with the TCO (transparent conductive oxide), and the presence of P-O species observed using the reflection–absorption infrared spectrum provides clear evidence that the interfacial bonding between evaporated 2PACz and ITO is consistent with that of solution-processed 2PACz [106]. Notably, this approach exhibited compatibility with textured surfaces and scalability for industrial production, making it a promising alternative to solution processing.

In addition, Qi et al. expanded the scope of vacuum deposition by comparing it with spray-coating and spin-coating for 2PACz deposition. They demonstrated that thermal evaporation not only improves layer uniformity and thickness control but also enhances the overall morphology and interfacial dipole alignment [109]. Such precision enables better energy level matching between SAMs and perovskite layers, improving device performance and scalability for larger modules [110]. From the perspective of processability over a textured surface, Kore et al. demonstrated the effectiveness of thermally evaporated SAMs in fully textured perovskite-silicon tandem devices. The study demonstrated the ability of vacuum deposition to produce conformal and defect-free SAM layers on challenging textured surfaces, which is critical for achieving high efficiency in tandem architectures (Figure 5c). By optimizing the thickness of evaporated SAM layers, they achieved PCEs exceeding 30% in lab-scale tandem devices, highlighting the scalability and industrial potential of this approach [108].

SAMs, such as 2PACz with its large dipole moment, are widely used as hole transport layers in inverted perovskite solar cells (PSCs) due to their efficient charge transfer properties, but their energy level alignment at interfaces remains underexplored [112]. In this context, Chen et al. comprehensively investigated the energy level alignment of

2PACz molecules on various substrates, leveraging the advantages of vacuum deposition to gain precise control over molecular orientation, which is critical for minimizing interfacial recombination and enhancing charge extraction (Figure 4b). This research found an influence on dipole moment, depending on molecule configuration. For example, on solvent-cleaned and plasma-treated ITO substrates, the SAM molecules assemble vertically, leading to an increase in work function. However, on sputtered ITO, the SAM molecules adopt an inverted orientation, significantly reducing work function (Figure 4c). These findings confirmed that vacuum-deposited SAMs provide superior interfacial properties to their solution-processed counterparts, especially when combined with surface treatments such as plasma cleaning or sputtering [110].

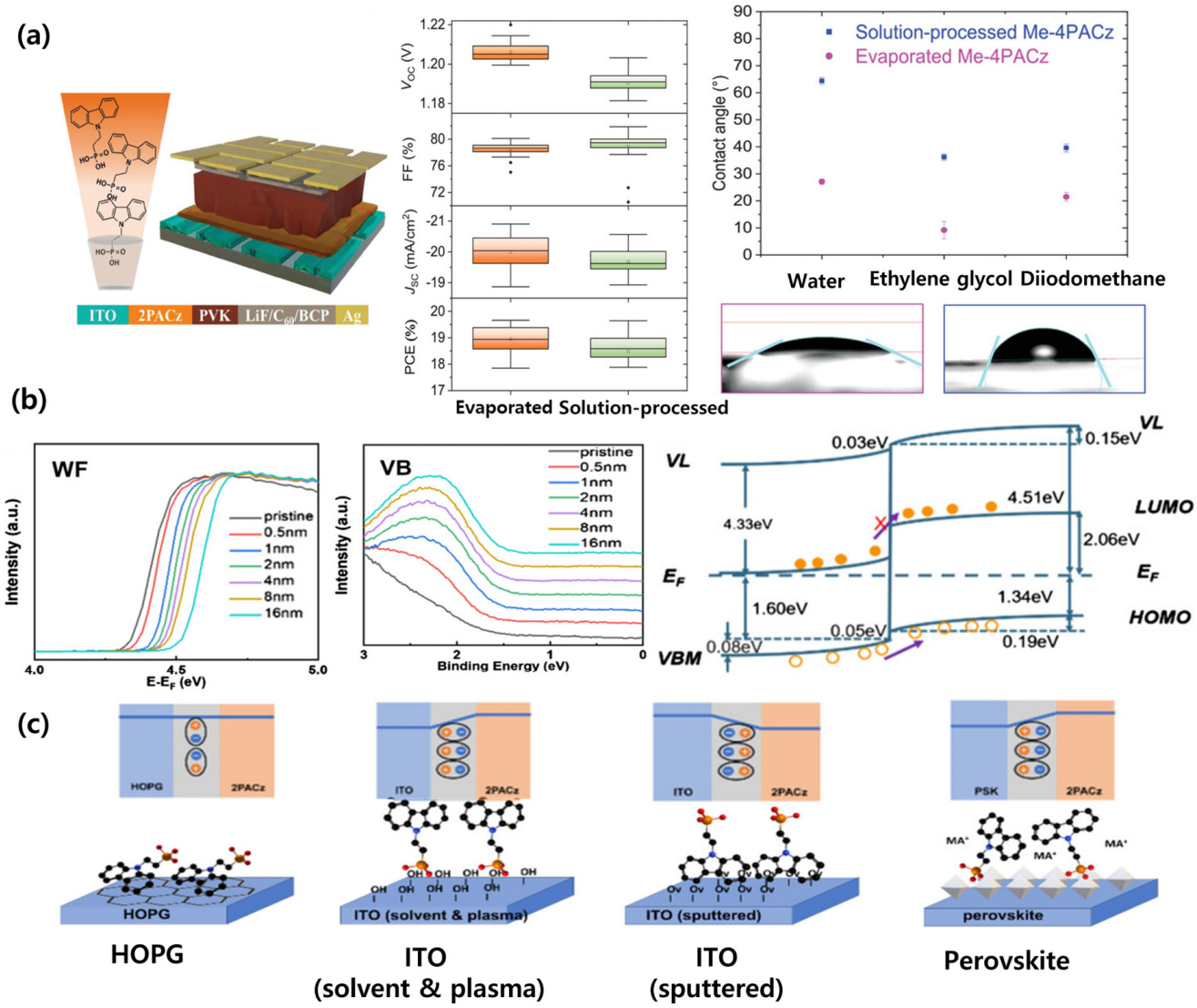


Figure 4. (**a**) Illustration of the perovskite device architecture with thermal vacuum deposition process and a comparative analysis of photovoltaic performance parameters of vacuum and solution-processed PSCs. Contact angle of vacuum deposition and solution-processed Me-4PACz and comparison of device performance using solution and evaporation process. permission from ref. [106] copyright 2024 Wiley. (**b**) Work function and valance band spectra of MAPbI3/2PACz interface with energy level diagram of MAPbI3 and 2PAC. (**c**) 2PACz molecule arrangement on various substrates and dipole interactions. Reproduced with permission from ref. [110], copyright 2025 Wiley.

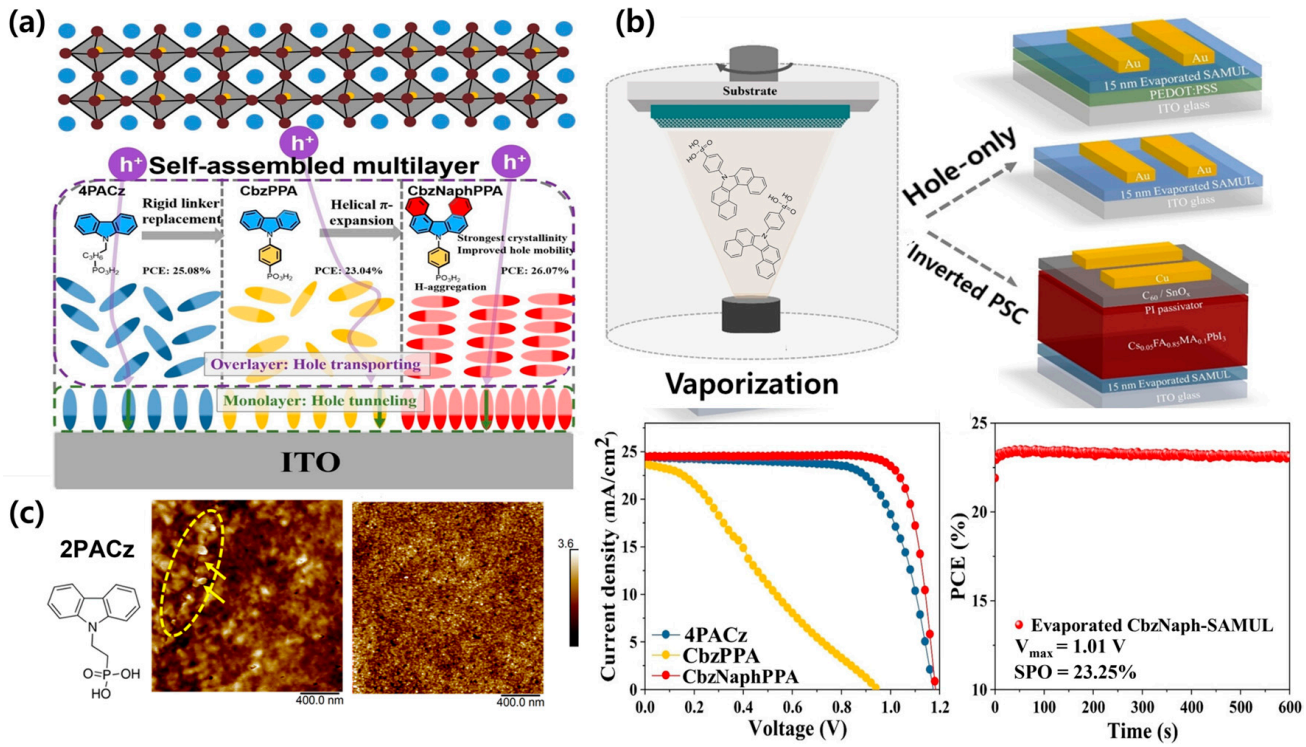


Figure 5. (**a**) Formation of overlayer and packing mechanism of 4PACz, CbzPPA, CbzNaphPPA in PSC. (**b**) CbzNaphPPA-based SAMUL device deposited using thermal vacuum deposition and the corresponding photovoltaic performance. Reproduced with permission from ref. [111], copyright 2024 Wiley. (**c**) Comparison of surface uniformity using thermal vacuum processed and solution-processed 2PACz. Reproduced with permission from ref. [108], copyright 2024 Royal Society of Chemistry.

In the case of vacuum deposition, fine control over the deposition thickness is achievable. However, the absence of a washing step often leads to the formation of disordered overlayers. These disordered layers, consisting of loosely packed SAM molecules, contribute to substrate coverage, improved wettability, and defect passivation [113]. However, a thicker overlayer should have efficient charge transporting ability for maintaining effective carrier extraction and minimizing recombination losses at the interface [114]. In this context, to enhance the performance of PSCs, a comprehensive understanding of the molecular structure–property–performance relationship is essential. Jen et al. introduced a novel self-assembled multilayer (SAMUL) structure fabricated using thermal evaporation, achieving highly ordered molecular packing and enhanced hole transport (Figure 5a). The SAMUL architecture demonstrated a significant increase in fill factor and power conversion efficiency (PCE), offering new opportunities for advanced PSC applications (Figure 5b). Specifically, the SAMUL structure was fabricated utilizing (4-(7H-dibenzocarbazol-7-yl) phenyl) phosphonic acid (CbzNaphPPA), a molecule with a rigid conjugated core and H-aggregation properties. This design improved molecular rigidity and intermolecular interactions, resulting in superior hole mobility and stability. Their work emphasized that the crystalline molecular arrangement within SAMULs is crucial for optimizing interfacial charge transport properties [111]. Additionally, the device-based CbzNaphPPA showed excellent device stability (94% of its initial PCE retained after continuous operation for 1200 h under 1-sun irradiation) compared to the solution-processed method (77% of its initial PCE retained after continuous operation for 1200 h under 1-sun irradiation). Another study on the stability of SAMs was conducted by Na et al., who demonstrated that vacuum deposition-based Me-4PACz promotes the formation of uniform perovskite films and enhances charge extraction and transfer at the perovskite interface. This approach resulted in

improved efficiency and stability compared to the solution-processed method. The PCE of the device with vacuum deposition-based Me-4PACz reached 20.31% and retained 87% of its initial PCE after 1144 h at 65 °C in an N_2 atmosphere. In contrast, the solution process device showed 18.44% PCE and retained 63% of its initial PCE after 1144 h at 65 °C in an N_2 atmosphere [53].

In conclusion, these studies thoroughly highlight the pioneering potential of vacuum-deposited SAMs in perovskite solar cells. By addressing the limitations of solution-based methods, vacuum deposition offers a robust, scalable, and high-precision approach to fabricating SAM layers with superior interfacial properties [115]. Additionally, the recent advancements in vacuum-deposited SAMs demonstrate their effectiveness in improving device performance, particularly in enhancing charge transport and interfacial stability. However, despite these advantages, several challenges must be addressed to fully unlock their potential. One of the critical challenges is the thermal stability of SAMs under high-temperature processing conditions. In particular, certain inorganic perovskite compositions necessitate a high-temperature annealing process above 200 °C, posing a significant challenge due to the thermal instability of SAMs [95]. For example, it is reported that Me-4PACz undergoes liquefaction at 200 °C, followed by a dehydration condensation reaction that transforms phosphonic acid groups into –P–O–P– bonds [116,117]. Therefore, future work should focus on optimizing vacuum deposition conditions and exploring the thermal stability of SAMs to fully realize their potential in advancing PSC technology.

4. Importance of Interaction Between SAM and Perovskite

The functional groups present in the molecular structure of SAMs play a crucial role in interfacial interactions with perovskite [88]. Specifically, groups such as methyl or methoxy can significantly impact the interfacial charge transfer rates, as well as charge extraction efficiency [12,20,118]. These modifications enable fine-tuning of the electronic properties at the interface, which is essential for optimizing the performance of perovskite-based devices. In addition, the interaction between the terminal group of SAM and perovskite is critical, as it directly affects the perovskite's lattice structure, crystallization, and surface properties, all of which influence device performance [14,76,119]. These interactions, including coordination bonding, van der Waals forces, and electrostatic interactions, enable SAMs to integrate into the perovskite lattice, improving wettability, crystallinity, and defect passivation [120]. By reducing trap states and minimizing non-radiative recombination, SAMs can enhance charge transport and promote uniform crystal growth, ultimately improving the stability and efficiency of perovskite-based technologies [74].

4.1. Surface Contact Behavior Between SAM and Perovskite

In perovskite solar cells, hydrophobic PTAA HTL introduces challenges due to its poor surface wettability upon exposure to the perovskite precursor solution [121–124]. To address the issue of interfacial defects, SAM-based HTL with tunable functional groups can be introduced to improve wettability and enhance interactions with the perovskite layer [125–128]. In this regard, the hydrophilic SAM can alter the surface properties of the SAM-based substrate by modifying the terminal groups of the SAM, thereby adjusting its hydrophilicity to enhance coating efficiency [128,129]. This modification also improves the quality of the coating of the perovskite.

To explore this strategy in detail, studies have focused on developing novel SAMs to enhance surface wettability and improve the deposition quality of perovskite films. Zhu et al. synthesized a new SAM—TPA-PT-C6—which contains two triarylamine groups on the phenothiazine core unit (both of which are excellent hole-extraction/transportation building blocks, but inherently hydrophobic) and a CA-Br, hydrophilic ammonium salt

containing co-adsorbent. In this study, the CA-Br, with its hydrophilic nature, modulated the surface properties of the hole-extracting layer (HEL) and improved the wettability of perovskite precursor on the self-assembled HEL, thus improving the morphology and quality of perovskite films (Figure 6a). They found that CA-Br mitigates the poor wettability issue that hampers large-area uniform perovskite deposition [129].

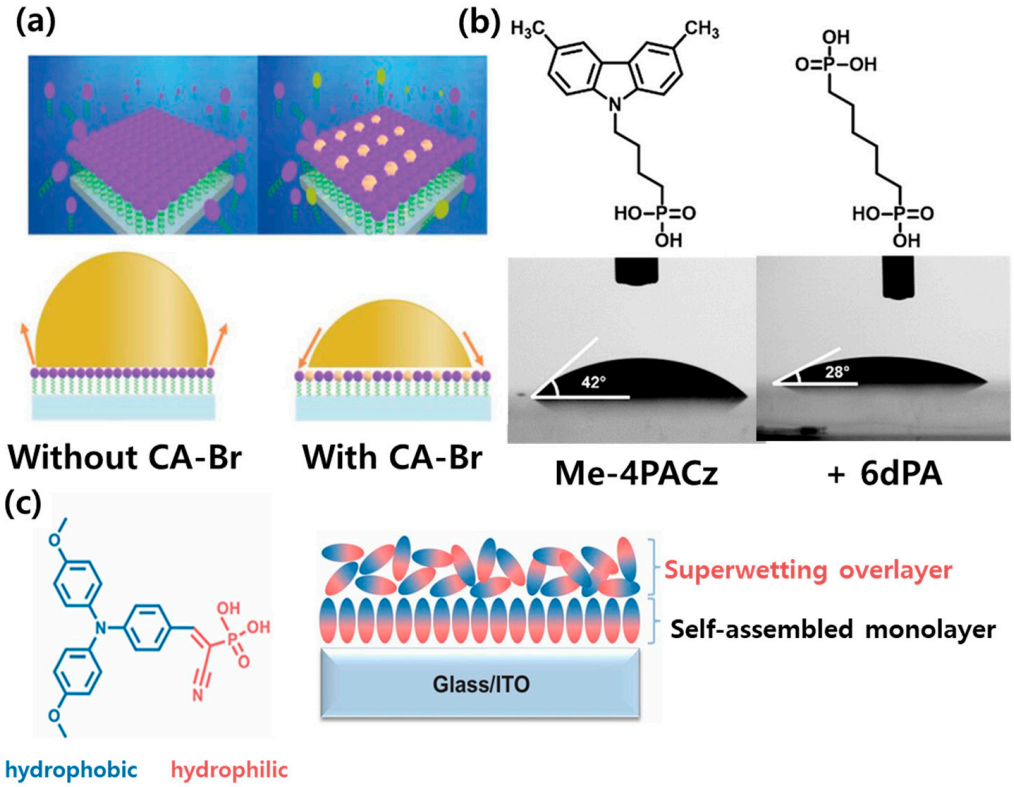


Figure 6. (**a**) Surface contact behavior depending on CA-Br. Reproduced with permission from ref. [129], copyright 2019 Wiley (**b**) Chemical structures of Me-4PACz and 6dPA and surface wettability difference by adding 6dPA. Reproduced with permission from ref. [113], copyright 2023 American Chemical Society. (**c**) Molecular structure of the amphiphilic MPA-CPA and schematic depiction of overlayer stack formation of MPA-CPA on the substrate. Reproduced with permission from ref. [114], copyright 2024 Science.

Similar strategies have also focused on improving the wettability of self-assembled monolayers (SAMs) for enhanced perovskite deposition. For example, Magomedov et al. addressed the poor wettability of Me-4PACz, a widely used hole-selective monolayer in PSCs, by introducing 1,6-hexylenediphosphonic acid (6dPA) as an additive to the monolayer precursor solution (Figure 6b). This modification significantly improved the surface energy of the SAM layer, particularly by increasing its polar component, which resulted in better surface coverage and reduced the contact angle of the perovskite precursor solution (from 42° for Me-4PACz monolayer to 28° for Me4PACz+6dPA monolayer). The improved wettability facilitated the formation of high-quality perovskite films with uniform coverage, even on large-area substrates (67% shunts onto the Me-4PACz monolayer vs. 8% shunts onto the Me4PACz+6dPA monolayer). Furthermore, the study demonstrated that the addition of 6dPA did not negatively impact device performance. As a result, devices fabricated with the Me-4PACz+6dPA monolayer achieved a PCE of 20.9% for small-area PSCs, while devices with a 1 cm^2 active area achieved a PCE of 18.7% [113]. These results highlight the potential scalability of the approach for larger-area devices, addressing a critical challenge in the commercialization of PSC technology.

Another study improved the amphiphilic properties of SAMs without the use of separate coadsorbents or additives. Wu et al. demonstrated the effectiveness of an amphiphilic molecular hole transporter, 2-(4-(bis(4-methoxyphenyl)amino) phenyl)-1-cyanovinyl)phosphonic acid (MPA-CPA), which has a hydrophilic CPA anchoring group and a hydrophobic methoxy-substituted triphenylamine (MPA) hole-extraction group. When a solution of MPA-CPA was spin-coated onto a glass–ITO substrate, it formed a bilayer structure comprising a chemically anchored SAM and an unabsorbed, disordered overlayer (Figure 6c). This overlayer exhibited super wetting properties towards the perovskite precursor solution, with a small contact angle (~5°), enhancing perovskite deposition, which was beneficial on larger-area substrates. In comparison, the contact angles for perovskite solutions on PTAA and 2PACz HTLs were higher, measuring 33.5° and 17.9°, respectively [114]. In this study, the overlayer played a crucial role in achieving super wetting properties, while a higher concentration of MPA-CPA in the spin-coating solution decreased the contact angle, enhancing wettability.

4.2. Perovskite Crystallization Depending on SAM

SAMs can also influence the growth process and quality of the perovskite film [52,130]. The crystallization of perovskite films generally occurs in two stages. The first phase involves perovskite nucleation, where perovskite seeds form on the substrate. During the subsequent drying and thermal annealing processes, these seeds undergo inter-diffusion, promoting the growth of perovskite grains through seed interactions [131]. To enhance grain size, it is essential to maintain sufficient spacing between perovskite seed crystals and ensure high mobility at the grain boundaries. SAMs can reduce the drag between the substrate and perovskite solution, facilitating the formation of larger grains [132,133]. In short, SAMs play a critical role in guiding the nucleation and growth processes, ultimately influencing the morphology and performance of perovskite films.

Building on the above understanding, Jen et al. designed two sulfur-substituted carbazole SAMs (Cbz2S and Cbz2SMe). Cbz2S incorporates a cyclic disulfide bond at the carbazole 4,5-positions, forming a heptacyclic ring. This structural configuration ensures that two sulfur atoms are positioned atop the SAM molecule, maximizing their exposure and creating a sulfur-rich surface on the ITO substrate. On the other hand, Cbz2SMe was derived through in situ ring opening and methylation of the disulfide bond, resulting in fewer exposed sulfur groups due to the steric hindrance from the methyl groups. In this study, the excessive exposure of Lewis-basic sulfur atoms in Cbz2S adversely affects perovskite crystallization, leading to suboptimal device performance (Figure 7a). The strong interaction between S and uncoordinated Pb^{2+} led to the accumulation of excessive Pb^{2+} at the buried interface, changing the compositional balance of the precisely formulated precursor. On the other hand, the surface created by Cbz2SMe, which is structurally tuned by masking partially exposed areas of sulfur atoms, effectively addressed this issue by partially shielding the exposed sulfur atoms. This modification delicately balances the crystallization of perovskite and the passivation of extra Pb^{2+}, thereby synergistically combining buried interface passivation with efficient hole-selective functionality. As a result, the optimized surface properties of Cbz2SMe enabled the fabrication of high-performance inverted perovskite solar cells (PSCs), achieving a remarkable power conversion efficiency of 24.42% along with enhanced long-term stability over 900 h under the ambient environment with 74% relative humidity [134].

Research has also been conducted in which SAMs complement existing HTLs by addressing their limitations and improving lattice disordering in the perovskite layer. Chen et al. utilized a bilayer of 2PACz on PEDOT:PSS in high-bandgap tin-based PSCs. Poly(3,4-ethenedioxythiophene): poly(styrenesulfonate) (PEDOT-PSS) is the most widely

used HTL in p-i-n structure PSCs because of its high optical transmittance and low-temperature fabrication process. However, its stability is far from satisfactory because of PSS's acidity, which damages the perovskite layers. They introduced a 2PACz monolayer deposited on the PEDOT-PSS layer, which energetically aligned the interface of the SAM/Sn-based perovskite, resulting in the lower lattice disordering and reduced non-radiative recombination in the perovskite layer (Figure 7b). Device stability was improved by the compact surface morphology of the Sn perovskite deposited on a bilayer structure of 2PACz monolayer on PEDOT-PSS, which effectively suppressed direct contact between PEDOT-PSS and perovskite film [135].

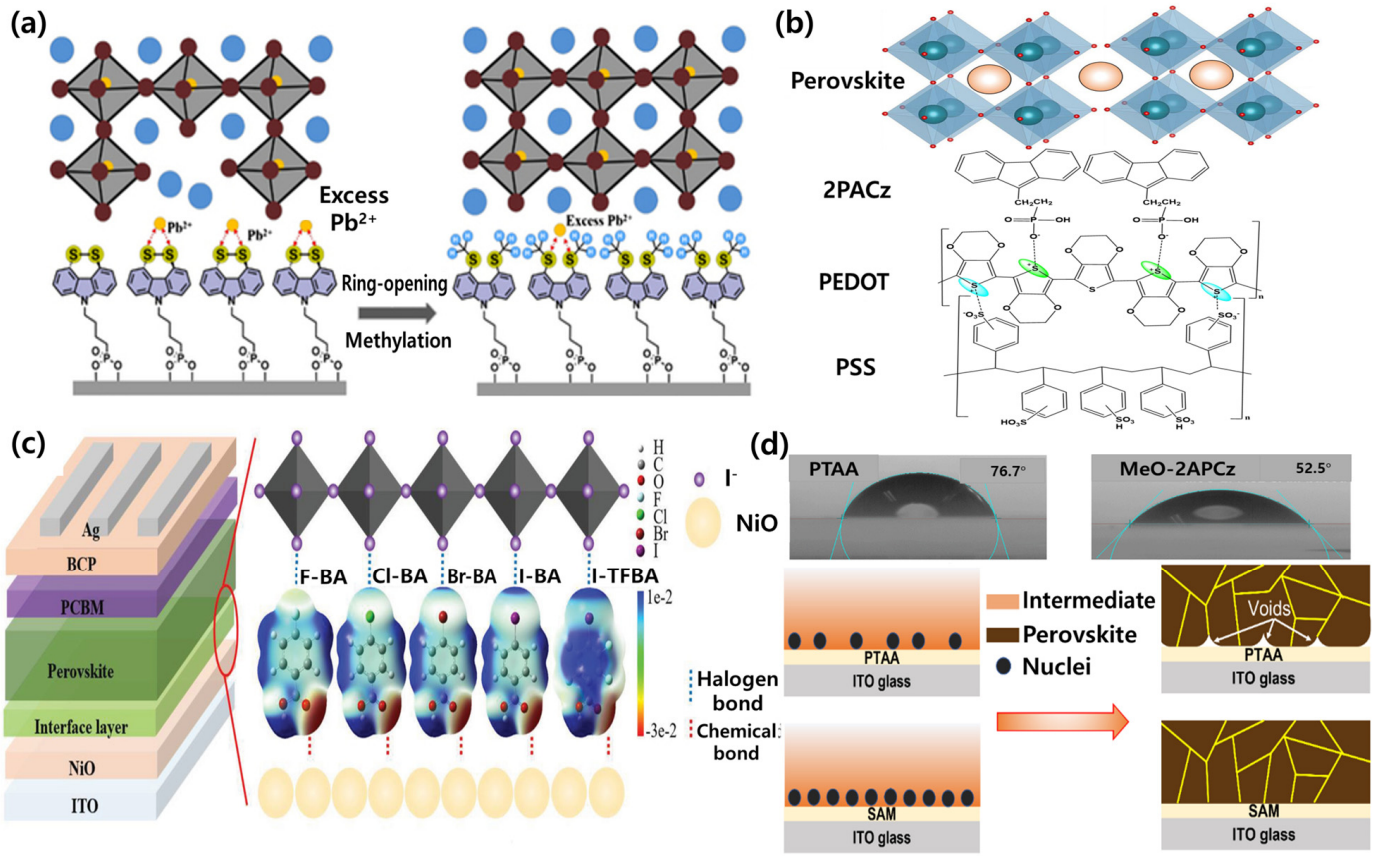


Figure 7. (**a**) Interaction of perovskite crystal with sulfur-substituted SAM (Cbz2S and Cbz2SMe). Reproduced with permission from ref. [134], copyright 2024 Chinese Chemical Society. (**b**) Coordinating interaction between perovskite layer and bilayer of 2PACz on PEDOT:PSS. Reproduced with permission from ref. [135], Copyright 2021 American Chemical Society. (**c**) Coordination interaction between SAMs and the perovskite layer. Reproduced with permission from ref. [77], copyright 2023 Wiley. (**d**) The contact angles of PTAA and MeO-2PACz SAM and their influence on the nucleation and growth of perovskite. Reproduced with permission from ref. [136], copyright 2022 Tsinghua University Press.

The impact of chemical interactions between SAMs and perovskite precursors on crystallization and charge transfer has also been explored using various approaches by other research groups. Kim et al. used three methoxybenzoic acid derivatives as a SAM to modify the perovskite crystallization. Among the derivatives, 3,4,5-trimethoxybenzoic acid (TMBA) showed strong dipole moment and hydrogen bonding with ammonium cations. This interaction improved charge transfer characteristics, enhanced perovskite crystallization, and facilitated interfacial charge transfer [64]. Chen et al. introduced 3-aminopropanoic acid (C3-SAM) to modify the substrate in perovskite solar cells (PSCs). The incorporation of C3-SAM not only improved the crystallinity of the perovskite film by reducing pinholes

and charge traps but also created an energetically aligned surface that enhanced charge extraction. This modification led to a significant performance enhancement, with the device efficiency increasing by 31%, from 11.96% to 15.67% [137].

Research has also been conducted on utilizing halogen functional groups to regulate crystallization behavior. Han's research team demonstrated that iodine atoms in 4-iodobenzoic acid (I-BA) and 4-iodo-2,3,5,6-tetrafluorobenzoic acid (I-TFBA) form strong halogen bonds with I^- ions in the perovskite layer. This interaction suppresses I_2 formation under continuous light exposure and prevents void formation at the interface (Figure 7c). Additionally, the directional halogen bonding promotes the oriented crystallization of the perovskite, enhancing charge transfer behavior. As a result, devices treated with I-TFBA achieved a high efficiency of 22.02% and maintained 91.9% of their initial PCE after 1000 h of light soaking at 55 °C, demonstrating improved stability [77].

Lastly, the impact on large-area applications has also been investigated. For example, Jen et al. used a blade-coating process to study the nucleation and growth of perovskite films, highlighting the influence of substrate wettability. On hydrophobic PTAA surfaces, nucleation is delayed, resulting in sparsely distributed nuclei with large gaps, leading to incomplete horizontal crystal growth. In contrast, hydrophilic SAM surfaces facilitate dense nucleation and uniform crystal growth in both vertical and horizontal directions (Figure 7d). Additionally, methoxy functional groups of MeO-2PACz SAMs improve adhesion by forming coordination bonds with Pb^{2+} ions [136].

4.3. Defect Passivation by SAM

The interaction between the terminal groups of SAM molecules and the perovskite layer affects the passivation of the perovskite interface [138–141]. The perovskite layer often contains surface or bulk defects, such as dangling bonds and ion vacancies, which can act as trap states, leading to charge recombination and reduced device efficiency [142–145]. SAMs can passivate these defects by chemically interacting with the perovskite surface, filling vacancies, and neutralizing surface states [120,146]. Through these defect-passivating interactions, SAMs contribute to improved stability by preventing degradation processes at the surface and enhancing the long-term durability of perovskite.

The overall result is a more efficient and stable interface, leading to better device performance in terms of both power conversion efficiency and operational lifetime [119,147]. Jen et al. reported MeO-BTBT-based SAMs with more extended conjugation and larger sulfur atoms compared to MeO-2PACz. These features induce strong intermolecular interactions with the perovskite layer and enable a more compact SAM layer on the ITO substrate. During the crystallization, the Lewis-basic sulfur atoms in the BTBT fused ring can coordinate with Pb^{2+} ions to effectively passivate the defects at the perovskite interface (Figure 8a). As a result, the incorporation of MeO-BTBT in PSCs achieved a PCE of 24.53% [139]. In addition, Takhellambam et al. introduced a C10-BTBT (2-decyl[1]benzothieno [3,2-b][1]benzothiophene) interlayer with improved charge transfer at the perovskite interface, resulting in a high PCE of 20.50% [27]. He et al. synthesized a dimethylacridine-SAM, DMAcPA, which contains two bromine (Br) substituents. DMAcPA was used for passivating grain boundaries and improving the perovskite/ITO contact. During the crystallization process, DMAcPA was extruded to the grain boundaries, where the steric effect of two methyl groups prevented aggregation and jamming at grain boundaries. The perovskite film doped with DMAcPA reduced deep-level hole trap density by suppressing defect states at the grain boundaries and surface (Figure 8b). As a result, PSCs with DMAcPA achieved a power conversion efficiency (PCE) of 25.86%, with a certified value of 25.39% [148]. Chen's group developed a self-assembled monolayer based on p-chlorobenzenesulfonic acid (CBSA) to reduce interfacial defects. The sulfonic acid groups

passivate surface oxygen defects in metal oxide, while chlorine atoms fill iodine vacancies in the lower perovskite layer (Figure 8c). This interlayer also relieves lattice strain in the bottom perovskite layer, reducing interfacial strain and preventing undesirable reactions at the perovskite interface [119].

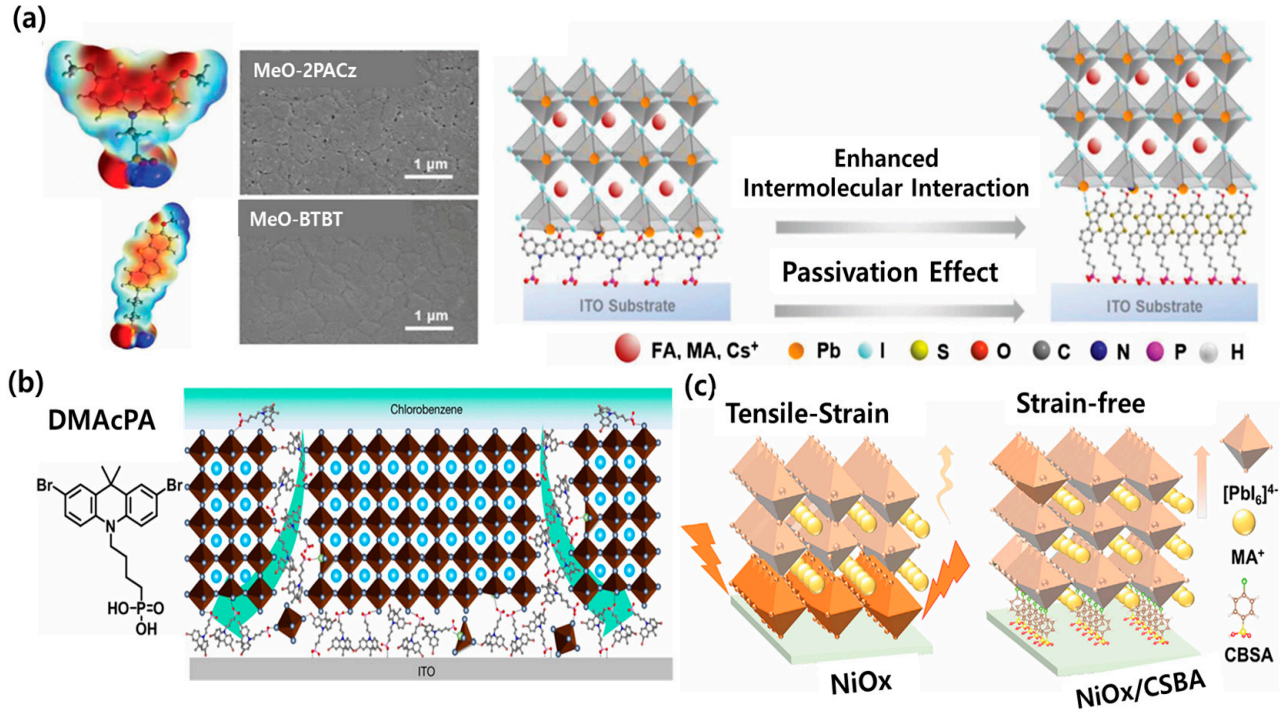


Figure 8. (**a**) SEM images of perovskite with SAM and electrostatic surface potential of MeO-2PACz and MeO-BTBT. Reproduced with permission from ref. [139], copyright 2024 Wiley. (**b**) Chemical structure of DMAcPA and defect passivation with perovskite grain boundaries. Reproduced with permission from ref. [148], copyright 2024 nature. (**c**) Schematic illustration of the tensile strain in perovskite lattice depending on the presence of CBSA. Reproduced with permission from ref. [119], copyright 2022 Wiley.

5. Perspective

Self-assembled monolayers (SAMs) undoubtedly represent an innovative approach to the cost-effective and high-performance development of PSC, owing to their versatile structural tunability and superior processing characteristics. Nevertheless, despite their numerous advantages, SAM materials still face significant challenges, especially regarding their deposition processability and stability, particularly for vacuum-processed SAMs. Additionally, the intricate chemical interactions between SAMs and perovskite layers, particularly their role in defect passivation and energy level alignment, have not been thoroughly explored. A deeper understanding of these fundamental mechanisms is essential for unlocking the full potential of SAMs and further enhancing their contribution to PSC efficiency improvements.

1. Vacuum deposition processability: Evaporation techniques for SAMs and perovskites have demonstrated significant potential in enhancing the performance of perovskite solar cells. Vacuum-deposited SAMs enable precise molecular ordering and uniform thin layers formation with physical adsorption. Therefore, it is suitable as a preceding process for vacuum-processed perovskite deposition. Despite these advantages, the SAM vacuum deposition process remains underexplored, requiring further investigation to address several critical challenges. In particular, the thermal stability of SAMs is a major concern, as the SAM layer tends to decompose at high temperatures. Therefore, studies focusing on enhancing the thermal stability of SAMs are

essential. Additionally, due to the formation of weaker physisorption compared to solution-based processing, post-deposition treatments are essential to improve the bonding strength.

2. Functional group interaction with perovskite: The interaction between the terminal group of the SAM and the perovskite directly influences the perovskite's lattice structure, crystallization process, and surface properties, which are key to enhancing the performance of perovskite-based devices. These interactions, which include coordination bonding, van der Waals forces, and electrostatic interactions, enable SAMs to integrate into the perovskite lattice structure. This incorporation can modify the perovskite's surface wettability and lattice crystallinity, affecting key factors like crystallization and defect passivation. Despite these advantages, the mechanisms underlying the enhancement of perovskite crystallinity, contact behavior, and passivation effects induced by the SAM layer remain poorly understood. Specifically, the interaction between the SAM layer and perovskite varies depending on the functional groups in the SAM. Therefore, developing functional groups that can enhance perovskite device performance is essential.

This review emphasizes that future research should prioritize the optimization of SAM deposition processes to achieve more uniform, compact, and stable layers that can significantly enhance the performance of perovskite solar cells. Furthermore, it is crucial to focus on the development of SAM functional groups that can effectively modify the perovskite crystallinity, surface contact behavior, and passivation effect. These interaction mechanisms are vital for improving interfacial charge transport, minimizing charge recombination, and ultimately enhancing the overall efficiency and stability of the device. By designing SAMs with vacuum processability and a range of functional groups, we can significantly improve the performance of perovskite solar cells and overcome some of the existing limitations of PSCs.

Funding: This work was supported by the research fund of Chungnam National University.

Data Availability Statement: No new data were created or analyzed in this study. Data sharing is not applicable to this article.

Conflicts of Interest: The authors declare no conflicts of interest.

References

1. Kim, I.B.; Kim, Y.J.; Kim, D.Y.; Jang, S.Y. A Thiophene Based Dopant-Free Hole-Transport Polymer for Efficient and Stable Perovskite Solar Cells. *Macromol. Res.* **2022**, *30*, 391–396. [CrossRef]
2. Park, J.Y.; Jang, J.W.; Shen, X.; Jang, J.H.; Kwak, S.L.; Choi, H.; Lee, B.R.; Hwang, D.H. Fluorene- and Arylamine-Based Photo-Crosslinkable Hole Transporting Polymer for Solution-Processed Perovskite and Organic Light-Emitting Diodes. *Macromol. Res.* **2023**, *31*, 721–732. [CrossRef]
3. Arivunithi, V.M.; Park, H.Y.; Reddy, S.S.; Do, Y.; Park, H.; Shin, E.S.; Noh, Y.Y.; Song, M.; Jin, S.H. Introducing an Organic Hole Transporting Material as a Bilayer to Improve the Efficiency and Stability of Perovskite Solar Cells. *Macromol. Res.* **2021**, *29*, 149–156. [CrossRef]
4. Lee, K.H.; Kim, D.Y.; Yang, S.Y. Surface Induced Porous Morphological Transition of the Organic Self-Assembled Monolayer Hybridized Polyelectrolyte Thin Films. *Macromol. Res.* **2013**, *21*, 127–129. [CrossRef]
5. Sery, A.A.; Abd El-Samad, A.E.; Mostafa, R.S.; Zeenelabden, H.H.; Elseman, A.M.; Sajid, S.; Rashad, M.M.; El-Aasser, M. Toward High-Performance Carbon-Based Perovskite Solar Cells. *Sol. Energy* **2025**, *287*, 113261. [CrossRef]
6. Liu, H.-S.; Huan, C.-M.; Xiao, X.-D.; Bi, Z.-N.; Lu, Y.; Qi, S.; Zhan, Y.-J.; Xu, X.-Q.; Xu, G. Research Progress of All-Inorganic Perovskite Solar Cells. *Adv. New Renew. Energy* **2019**, *7*, 142–148.
7. Yuan, S.-Y.; Li, Z.-Z.; Wang, Y.-T.; Zhao, H. CsPbI3 All-Inorganic Perovskite Solar Cells: Development Status and Theoretical Prediction. *J. Solid State Chem.* **2024**, *336*, 124780. [CrossRef]
8. Afre, R.A.; Pugliese, D. Perovskite Solar Cells: A Review of the Latest Advances in Materials, Fabrication Techniques, and Stability Enhancement Strategies. *Micromachines* **2024**, *15*, 192. [CrossRef]

9. Goni, L.K.M.O.; Abdur, R.; Hossain, M.; Chowdhury, S.; Shahinuzzaman, M.; Shaikh, M.A.A.; Jamal, M.S. Exploring the Impact of Halide Composition on Stability and Power Conversion Efficiency in All-Inorganic Perovskite Solar Cells. *J. Mater. Sci.* **2024**, *59*, 18279–18315.
10. Sharif, R.; Khalid, A.; Ahmad, S.W.; Rehman, A.; Qutab, H.G.; Akhtar, H.H.; Mahmood, K.; Afzal, S.; Saleem, F. A Comprehensive Review of the Current Progresses and Material Advances in Perovskite Solar Cells. *Nanoscale Adv.* **2023**, *5*, 3803–3833. [CrossRef]
11. Wang, Y.; Ye, J.; Song, J.; Cao, J.; Zhou, P.; Xu, X.; Zhou, Q.; Li, G.; Tu, Y.; Chu, L.; et al. Synchronous Modulation of Hole-Selective Self-Assembled Monolayer and Buried Interface for Inverted Perovskite Solar Cells. *Cell Rep. Phys. Sci.* **2024**, *5*, 101992. [CrossRef]
12. Kim, S.Y.; Cho, S.J.; Byeon, S.E.; He, X.; Yoon, H.J. Self-Assembled Monolayers as Interface Engineering Nanomaterials in Perovskite Solar Cells. *Adv. Energy Mater.* **2020**, *10*, 2002606. [CrossRef]
13. Park, S.M.; Wei, M.; Lempesis, N.; Yu, W.; Hossain, T.; Agosta, L.; Carnevali, V.; Atapattu, H.R.; Serles, P.; Eickemeyer, F.T.; et al. Low-Loss Contacts on Textured Substrates for Inverted Perovskite Solar Cells. *Nature* **2023**, *624*, 289–294. [CrossRef]
14. Yu, X.; Sun, X.; Zhu, Z.; Li, Z. Stabilization Strategies of Buried Interface for Efficient SAM-Based Inverted Perovskite Solar Cells. *Angew. Chem.-Int. Ed.* **2024**, *64*, e202419608. [CrossRef]
15. Er-Raji, O.; Lange, S.; Hartwig, C.E.; Prasetio, A.; Bivour, M.; Hermle, M.; Turek, M.; De Wolf, S.; Glunz, S.W.; Borchert, J.; et al. Tuning Self-Assembly of Hole-Selective Monolayers for Reproducible Perovskite/Silicon Tandem Solar Cells. *Small Methods* **2025**, 2401758. [CrossRef]
16. Casalini, S.; Bortolotti, C.A.; Leonardi, F.; Biscarini, F. Self-Assembled Monolayers in Organic Electronics. *Chem. Soc. Rev.* **2017**, *46*, 40–71. [CrossRef] [PubMed]
17. Lan, Z.R.; Shao, J.Y.; Zhong, Y.W. Self-Assembled Monolayers as Hole-Transporting Materials for Inverted Perovskite Solar Cells. *Mol. Syst. Des. Eng.* **2023**, *8*, 1440–1455. [CrossRef]
18. Yi, Z.; Li, X.; Xiong, Y.; Shen, G.; Zhang, W.; Huang, Y.; Jiang, Q.; Ng, X.R.; Luo, Y.; Zheng, J.; et al. Self-assembled Monolayers (SAMs) in Inverted Perovskite Solar Cells and Their Tandem Photovoltaics Application. *Interdiscip. Mater.* **2024**, *3*, 203–244. [CrossRef]
19. Yeo, D.; Shin, J.; Kim, D.; Jaung, J.Y.; Jung, I.H. Self-Assembled Monolayer-Based Hole-Transporting Materials for Perovskite Solar Cells. *Nanomaterials* **2024**, *14*, 175. [CrossRef]
20. Liu, S.; Li, J.; Xiao, W.; Chen, R.; Sun, Z.; Zhang, Y.; Lei, X.; Hu, S.; Kober-Czerny, M.; Wang, J.; et al. Buried Interface Molecular Hybrid for Inverted Perovskite Solar Cells. *Nature* **2024**, *632*, 536–542. [CrossRef]
21. Choi, K.; Choi, H.; Min, J.; Kim, T.; Kim, D.; Son, S.Y.; Kim, G.W.; Choi, J.; Park, T. A Short Review on Interface Engineering of Perovskite Solar Cells: A Self-Assembled Monolayer and Its Roles. *Sol. RRL* **2020**, *4*, 1900251. [CrossRef]
22. Wang, S.; Guo, H.; Wu, Y. Advantages and Challenges of Self-Assembled Monolayer as a Hole-Selective Contact for Perovskite Solar Cells. *Mater. Futures* **2023**, *2*, 012105. [CrossRef]
23. Wu, Y.; Huang, Z.; Li, Q.; Yang, C.; Zhan, S.; Jia, X.; Li, C.; Islam, M.R.; Wang, Z.; Yue, S.; et al. Comprehensively Evaluating Feasibility of Self-Assembled Materials Applied to Hole Transport Layer for Commercializing Perovskite Solar Cells. *Mater. Res. Bull.* **2023**, *165*, 112327. [CrossRef]
24. Kim, G.; Kim, H.; Kim, M.; Sin, J.; Kim, M.; Kim, J.; Zhou, H.; Kang, S.H.; Oh, H.M.; Yang, J.Y. Enhancing Surface Modification and Carrier Extraction in Inverted Perovskite Solar Cells via Self-Assembled Monolayers. *Nanomaterials* **2024**, *14*, 214. [CrossRef] [PubMed]
25. Tang, H.; Shen, Z.; Shen, Y.; Yan, G.; Wang, Y.; Han, Q.; Han, L. Reinforcing Self-Assembly of Hole Transport Molecules for Stable Inverted Perovskite Solar Cells. *Science* **2024**, *383*, 1236–1240. [CrossRef] [PubMed]
26. Li, M.; Liu, M.; Qi, F.; Lin, F.R.; Jen, A.K.Y. Self-Assembled Monolayers for Interfacial Engineering in Solution-Processed Thin-Film Electronic Devices: Design, Fabrication, and Applications. *Chem. Rev.* **2024**, *124*, 2138–2204. [CrossRef]
27. Takhellambam, D.; Castriotta, L.A.; Zanotti, G.; Mancini, L.; Raglione, V.; Mattioli, G.; Paci, B.; Generosi, A.; Guaragno, M.; Campanari, V.; et al. Enhancing Hole Transfer in Perovskite Solar Cell with Self-Assembled Monolayer by Introducing [1]Benzothieno [3,2-*b*][1]Benzothiophene Interlayer. *Sol. RRL* **2023**, *7*, 2300658. [CrossRef]
28. Levine, I.; Al-Ashouri, A.; Musiienko, A.; Hempel, H.; Magomedov, A.; Drevilkauskaite, A.; Getautis, V.; Menzel, D.; Hinrichs, K.; Unold, T.; et al. Charge Transfer Rates and Electron Trapping at Buried Interfaces of Perovskite Solar Cells. *Joule* **2021**, *5*, 2915–2933. [CrossRef]
29. Al-Ashouri, A.; Magomedov, A.; Roß, M.; Jošt, M.; Talaikis, M.; Chistiakova, G.; Bertram, T.; Márquez, J.A.; Köhnen, E.; Kasparavičius, E.; et al. Conformal Monolayer Contacts with Lossless Interfaces for Perovskite Single Junction and Monolithic Tandem Solar Cells. *Energy Environ. Sci.* **2019**, *12*, 3356–3369. [CrossRef]
30. Pitaro, M.; Alonso, J.E.S.; Di Mario, L.; Romero, D.G.; Tran, K.; Kardula, J.; Zaharia, T.; Johansson, M.B.; Johansson, E.M.J.; Chiechi, R.C.; et al. Tuning the Surface Energy of Hole Transport Layers Based on Carbazole Self-Assembled Monolayers for Highly Efficient Sn/Pb Perovskite Solar Cells. *Adv. Funct. Mater.* **2023**, *34*, 2306571. [CrossRef]
31. Peng, C.; Huang, H.; Liu, W.; Zhang, Z.; Xu, Y.; Chen, S.; Li, S.; Du, S.; Wang, S.; He, Z.; et al. Reinforcement of Carbazole-Based Self-Assembled Monolayers in Inverted Perovskite Solar Cells. *ACS Appl. Mater. Interfaces* **2025**, *17*, 10745–10754. [CrossRef] [PubMed]

32. Zhou, H.; Wang, W.; Duan, Y.; Sun, R.; Li, Y.; Xie, Z.; Xu, D.; Wu, M.; Wang, Y.; Li, H.; et al. Glycol Monomethyl Ether-Substituted Carbazolyl Hole-Transporting Material for Stable Inverted Perovskite Solar Cells with Efficiency of 25.52%. *Angew. Chem.-Int. Ed.* **2024**, *63*, e202403068. [CrossRef]
33. Pitaro, M.; Alonso, J.S.; Di Mario, L.; Romero, D.G.; Tran, K.; Zaharia, T.; Johansson, M.B.; Johansson, E.M.J.; Loi, M.A. A Carbazole-Based Self-Assembled Monolayer as the Hole Transport Layer for Efficient and Stable $Cs_{0.25}FA_{0.75}Sn_{0.5}Pb_{0.5}I_3$ Solar Cells. *J. Mater. Chem. A* **2023**, *11*, 11755–11766. [CrossRef]
34. Li, W.; Martínez-Ferrero, E.; Palomares, E. Self-Assembled Molecules as Selective Contacts for Efficient and Stable Perovskite Solar Cells. *Mater. Chem. Front.* **2023**, *8*, 681–699. [CrossRef]
35. Huang, S.; Liang, C.; Lin, Z. Application of PACz-Based Self-Assembled Monolayer Materials in Efficient Perovskite Solar Cells. *ACS Appl. Mater. Interfaces* **2024**, *16*, 64424–64446. [CrossRef]
36. Peng, H.; Zheng, W.; Kim, G.Y.; Lee, J.W. Self-Assembled Monolayers as Hole-Selective Contacts in Inverted Perovskite Solar Cells: A Review. *Korean J. Chem. Eng.* **2024**, *41*, 3717–3735. [CrossRef]
37. Kasparavičius, E.; Franckevičius, M.; Driukas, S.; Gulbinas, V. Charge Carrier Dynamics at the Perovskite Interface with Self-Assembled Monolayers. *ACS Appl. Mater. Interfaces* **2024**, *16*, 59477–59487. [CrossRef]
38. Chen, J.; Park, N.G. Materials and Methods for Interface Engineering toward Stable and Efficient Perovskite Solar Cells. *ACS Energy Lett.* **2020**, *5*, 2742–2786. [CrossRef]
39. Wang, Y.; Jiang, W.; Liu, S.C.; Lin, C.T.; Fan, B.; Li, Y.; Gao, H.; Liu, M.; Lin, F.R.; Jen, A.K.Y. Durable Organic Photovoltaics Enabled by a Morphology-Stabilizing Hole-Selective Self-Assembled Monolayer. *Adv. Energy Mater.* **2024**, *14*, 2303354. [CrossRef]
40. Li, W.; Li, T.; Tong, Y.; Li, Y.; Wang, H.; Qi, H.; Wang, K.; Wang, H. Reducing Nonradiative Losses of Air-Processed Perovskite Films via Interface Modification for Bright and Efficient Light Emitting Diodes. *Adv. Funct. Mater.* **2024**, *34*, 2311133. [CrossRef]
41. Shih, C.J.; Chen, Y.S.; Luo, D.; Yu, C.W.; Chen, K.H.; Murokinas, G.; Huang, Y.C.; Li, C.F.; Huang, Y.C.; Liu, S.W. Exploring Buried Interface in All-Vapor-Deposited Perovskite Photovoltaics. *Sol. Energy* **2024**, *280*, 112872. [CrossRef]
42. Lee, K.C.; Kim, S.; Son, J.; Kong, J.; Yang, C. A Brief Review on Self-Assembled Monolayers in Organic Solar Cells: Progress, Challenges, and Future Prospects. *ACS Appl. Electron. Mater.* **2025**, *7*, 946–963. [CrossRef]
43. Diercks, A.; Petry, J.; Feeney, T.; Singh, R.; Zhao, T.; Hu, H.; Li, Y.; Paetzold, U.W.; Fassl, P. Sequential Evaporation of Inverted FAPbI3 Perovskite Solar Cells—Impact of Substrate on Crystallization and Film Formation. *ACS Energy Lett.* **2025**, *10*, 1165–1173. [CrossRef]
44. Liu, Y.; Ji, D.; Hu, W. Recent Progress of Interface Self-Assembled Monolayers Engineering Organic Optoelectronic Devices. *DeCarbon* **2024**, *3*, 100035. [CrossRef]
45. Li, M.; Xie, Y.; Lin, F.R.; Li, Z.; Yang, S.; Jen, A.K.Y. Self-Assembled Monolayers as Emerging Hole-Selective Layers Enable High-Performance Thin-Film Solar Cells. *Innovation* **2023**, *4*, 100369. [CrossRef]
46. Ren, Z.; Cui, Z.; Shi, X.; Wang, L.; Dou, Y.; Wang, F.; Lin, H.; Yan, H.; Chen, S. Poly(Carbazole Phosphonic Acid) as a Versatile Hole-Transporting Material for p-i-n Perovskite Solar Cells and Modules. *Joule* **2023**, *7*, 2894–2904. [CrossRef]
47. Chen, Q.; Sun, K.; Franco, L.R.; Wu, J.; Öhrström, L.; Liu, X.; Gumbo, M.; Ozório, M.S.; Araujo, C.M.; Zhang, G.; et al. Effects of Alkyl Spacer Length in Carbazole-Based Self-Assembled Monolayer Materials on Molecular Conformation and Organic Solar Cell Performance. *Adv. Sci.* **2024**, *12*, 2410277. [CrossRef]
48. Han, F.; Tu, Z.; Wan, Z.; Luo, J.; Xia, J.; Hao, G.; Yi, Y.; Wang, R.; Jia, C. Effect of Functional Group Position Change of Pyridinesulfonic Acid as Interface-Modified Layer on Perovskite Solar Cell. *Appl. Surf. Sci.* **2018**, *462*, 517–525. [CrossRef]
49. Arkan, E.; Unal, M.; Yalcin, E.; Arkan, M.Z.Y.; Yurtdas, S.; Can, M.; Tozlu, C.; Demic, S. Influence of End Groups Variation of Self Assembled Monolayers on Performance of Planar Perovskite Solar Cells by Interface Regulation. *Mater. Sci. Semicond. Process.* **2021**, *123*, 105514. [CrossRef]
50. Arkan, E.; Yalcin, E.; Unal, M.; Arkan, M.Z.Y.; Can, M.; Tozlu, C.; Demic, S. Effect of Functional Groups of Self Assembled Monolayer Molecules on the Performance of Inverted Perovskite Solar Cell. *Mater. Chem. Phys.* **2020**, *254*, 123435. [CrossRef]
51. Dai, Z.; Yadavalli, S.K.; Chen, M.; Abbaspourtamijani, A.; Qi, Y.; Padture, N.P. Interfacial Toughening with Self-Assembled Monolayers Enhances Perovskite Solar Cell Reliability. *Science* **2021**, *372*, 618–622. [CrossRef]
52. Anizelli, H.; David, T.W.; Tyagi, P.; Laureto, E.; Kettle, J. Enhancing the Stability of Perovskite Solar Cells through Functionalisation of Metal Oxide Transport Layers with Self-Assembled Monolayers. *Sol. Energy* **2020**, *203*, 157–163. [CrossRef]
53. Suo, J.; Yang, B.; Bogachuk, D.; Boschloo, G.; Hagfeldt, A. The Dual Use of SAM Molecules for Efficient and Stable Perovskite Solar Cells. *Adv. Energy Mater.* **2024**, *15*, 2400205. [CrossRef]
54. Kim, D.H.; Lee, H.J.; Lee, S.H.; Kang, Y.J.; Kwon, S.N.; Kim, D.H.; Na, S.I. Mixed Self-Assembled Hole-Transport Monolayer Enables Simultaneous Improvement of Efficiency and Stability of Perovskite Solar Cells. *Sol. RRL* **2024**, *8*, 2400067. [CrossRef]
55. Li, C.; Chen, Y.; Li, Y.; Gong, L.; Yuan, Z.; Liang, L.; Chen, J.; Ganesan, P.; Zhang, Y.; Ma, J.; et al. Deciphering the Impact of Aromatic Linkers in Self-Assembled Monolayers on the Performance of Monolithic Perovskite/Si Tandem Photovoltaic. *Angew. Chem.-Int. Ed.* **2024**, *64*, e202420585. [CrossRef]

56. Lenaers, S.; Lammar, S.; Krishna, A.; Stacchini, V.; Cardeynaels, T.; Penxten, H.; Weijtens, C.; Verhage, M.; Ruttens, B.; Maes, W.; et al. Pyrene-Based Self-Assembled Monolayer with Improved Surface Coverage and Energy Level Alignment for Perovskite Solar Cells. *Adv. Funct. Mater.* **2024**, 2411922. [CrossRef]
57. Li, C.; Zhang, Z.; Zhang, H.; Yan, W.; Li, Y.; Liang, L.; Yu, W.; Yu, X.; Wang, Y.; Yang, Y.; et al. Fully Aromatic Self-Assembled Hole-Selective Layer toward Efficient Inverted Wide-Bandgap Perovskite Solar Cells with Ultraviolet Resistance. *Angew. Chem.-Int. Ed.* **2024**, *63*, e202315281. [CrossRef]
58. Galvis, C.E.P.; Ruiz, D.A.G.; Martínez-Ferrero, E.; Palomares, E. Challenges in the Design and Synthesis of Self-Assembling Molecules as Selective Contacts in Perovskite Solar Cells. *Chem. Sci.* **2023**, *15*, 1534–1556. [CrossRef]
59. Li, M.; Li, Z.; Liu, M.; Fu, H.; Qi, F.; Lin, F.R.; Walsh, A.; Jen, A.K.Y. A Hole-Selective Self-Assembled Monolayer for Both Efficient Perovskite and Organic Solar Cells. *Langmuir* **2024**, *40*, 4772–4778. [CrossRef]
60. Liu, L.; Yang, Y.; Du, M.; Cao, Y.; Ren, X.; Zhang, L.; Wang, H.; Zhao, S.; Wang, K.; Liu, S. Self-Assembled Amphiphilic Monolayer for Efficient and Stable Wide-Bandgap Perovskite Solar Cells. *Adv. Energy Mater.* **2023**, *13*, 2202802. [CrossRef]
61. Zhang, Z.; Zhu, R.; Tang, Y.; Su, Z.; Hu, S.; Zhang, X.; Zhang, J.; Zhao, J.; Xue, Y.; Gao, X.; et al. Anchoring Charge Selective Self-Assembled Monolayers for Tin–Lead Perovskite Solar Cells. *Adv. Mater.* **2024**, *36*, e2312264. [CrossRef]
62. Baek, M.G.; Shin, J.E.; Park, S.G. Differences in ITO Interface Characteristics Change According to the Formation of Aromatic-Ring and Aliphatic Self-Assembled Monolayers. *Crystals* **2021**, *11*, 26. [CrossRef]
63. Hotchkiss, P.J.; Jones, S.C.; Paniagua, S.A.; Sharma, A.; Kippelen, B.; Armstrong, N.R.; Marder, S.R. The Modification of Indium Tin Oxide with Phosphonic Acids: Mechanism of Binding, Tuning of Surface Properties, and Potential for Use in Organic Electronic Applications. *Acc. Chem. Res.* **2012**, *45*, 337–346. [CrossRef] [PubMed]
64. Han, J.; Kwon, H.; Kim, E.; Kim, D.W.; Son, H.J.; Kim, D.H. Interfacial Engineering of a ZnO Electron Transporting Layer Using Self-Assembled Monolayers for High Performance and Stable Perovskite Solar Cells. *J. Mater. Chem. A* **2020**, *8*, 2105–2113. [CrossRef]
65. Li, E.; Liu, C.; Lin, H.; Xu, X.; Liu, S.; Zhang, S.; Yu, M.; Cao, X.M.; Wu, Y.; Zhu, W.H. Bonding Strength Regulates Anchoring-Based Self-Assembly Monolayers for Efficient and Stable Perovskite Solar Cells. *Adv. Funct. Mater.* **2021**, *31*, 2103847. [CrossRef]
66. Li, J.; Yuan, Y.J. Physisorption and Chemisorption of a Self-Assembled Monolayer by the Quartz Crystal Microbalance. *Langmuir* **2014**, *30*, 9637–9642. [CrossRef]
67. Dai, Z.; You, S.; Chakraborty, D.; Li, S.; Zhang, Y.; Ranka, A.; Barlow, S.; Berry, J.J.; Marder, S.R.; Guo, P.; et al. Connecting Interfacial Mechanical Adhesion, Efficiency, and Operational Stability in High Performance Inverted Perovskite Solar Cells. *ACS Energy Lett.* **2024**, *9*, 1880–1887. [CrossRef]
68. Mingorance, A.; Xie, H.; Kim, H.S.; Wang, Z.; Balsells, M.; Morales-Melgares, A.; Domingo, N.; Kazuteru, N.; Tress, W.; Fraxedas, J.; et al. Interfacial Engineering of Metal Oxides for Highly Stable Halide Perovskite Solar Cells. *Adv. Mater. Interfaces* **2018**, *5*, 1800367. [CrossRef]
69. Kreuzer, H.J.; Wang, R.L.C.; Grunze, M. Hydroxide Ion Adsorption on Self-Assembled Monolayers. *J. Am. Chem. Soc.* **2003**, *125*, 8384–8389. [CrossRef]
70. Fakult, D.T.; Universit, F. Hierarchical Assemblies of Core-Shell Metal Oxide Nanomaterials via Amide Coupling Reactions Hierarchische Anordnungen von Kern-Schale Metalloxid Nanomaterialien Über Amid-Kupplungsreaktionen. Ph.D. Thesis, University of Erlangen-Nuremberg, Erlangen, Germany, 2022.
71. Zhang, S.; Wu, R.; Mu, C.; Wang, Y.; Han, L.; Wu, Y.; Zhu, W.H. Conjugated Self-Assembled Monolayer as Stable Hole-Selective Contact for Inverted Perovskite Solar Cells. *ACS Mater. Lett.* **2022**, *4*, 1976–1983. [CrossRef]
72. Wang, G.; Chen, K.; Cheng, L.; Wang, D.; Meng, F.; Xiang, W. Application of Hole-Selective Self-Assembled Monolayers in Inverted Perovskite Solar Cells. *Sol. RRL* **2024**, *8*, 2300996. [CrossRef]
73. Lim, M.S.; Feng, K.; Chen, X.; Wu, N.; Raman, A.; Nightingale, J.; Gawalt, E.S.; Korakakis, D.; Hornak, L.A.; Timperman, A.T. Adsorption and Desorption of Stearic Acid Self-Assembled Monolayers on Aluminum Oxide. *Langmuir* **2007**, *23*, 2444–2452. [CrossRef] [PubMed]
74. Li, C.; Li, Y.; Chen, Y.; Zhang, H.; Zhang, S.T.; Zhang, Z.; Lin, F.; Liang, L.; Gong, L.; Hao, H.; et al. Enhancing Efficiency of Industrially-Compatible Monolithic Perovskite/Silicon Tandem Solar Cells with Dually-Mixed Self-Assembled Monolayers. *Adv. Funct. Mater.* **2024**, *34*, 2407805. [CrossRef]
75. Feeney, T.; Petry, J.; Torche, A.; Hauschild, D.; Hacene, B.; Wansorra, C.; Diercks, A.; Ernst, M.; Weinhardt, L.; Heske, C.; et al. Understanding and Exploiting Interfacial Interactions between Phosphonic Acid Functional Groups and Co-Evaporated Perovskites. *Matter* **2024**, *7*, 2066–2090. [CrossRef]
76. Abate, S.Y.; Huang, D.C.; Tao, Y.T. Surface Modification of TiO2 Layer with Phosphonic Acid Monolayer in Perovskite Solar Cells: Effect of Chain Length and Terminal Functional Group. *Org. Electron.* **2020**, *78*, 105583. [CrossRef]
77. Zhang, C.; Shen, X.; Chen, M.; Zhao, Y.; Lin, X.; Qin, Z.; Wang, Y.; Han, L. Constructing a Stable and Efficient Buried Heterojunction via Halogen Bonding for Inverted Perovskite Solar Cells. *Adv. Energy Mater.* **2023**, *13*, 2203250. [CrossRef]

78. Hung, C.M.; Mai, C.L.; Wu, C.C.; Chen, B.H.; Lu, C.H.; Chu, C.C.; Wang, M.C.; Yang, S.D.; Chen, H.C.; Yeh, C.Y.; et al. Self-Assembled Monolayers of Bi-Functionalized Porphyrins: A Novel Class of Hole-Layer-Coordinating Perovskites and Indium Tin Oxide in Inverted Solar Cells. *Angew. Chem.-Int. Ed.* **2023**, *62*, e202309831. [CrossRef]
79. Xu, Y.; Musgrave, C.B. A DFT Study of the Al2O3 Atomic Layer Deposition on SAMs: Effect of SAM Termination. *Chem. Mater.* **2004**, *16*, 646–653. [CrossRef]
80. Fürer, S.O.; Rietwyk, K.J.; Pulvirenti, F.; McMeekin, D.P.; Surmiak, M.A.; Raga, S.R.; Mao, W.; Lin, X.; Hora, Y.; Wang, J.; et al. Naphthalene-Imide Self-Assembled Monolayers as a Surface Modification of ITO for Improved Thermal Stability of Perovskite Solar Cells. *ACS Appl. Energy Mater.* **2023**, *6*, 667–677. [CrossRef]
81. Cao, Q.; Wang, T.; Pu, X.; He, X.; Xiao, M.; Chen, H.; Zhuang, L.; Wei, Q.; Loi, H.L.; Guo, P.; et al. Co-Self-Assembled Monolayers Modified NiOx for Stable Inverted Perovskite Solar Cells. *Adv. Mater.* **2024**, *36*, e2311970. [CrossRef]
82. Zhang, C.; Das, S.; Sakurai, N.; Imaizumi, T.; Sanjayan, S.; Shoji, Y.; Fukushima, T.; Zharnikov, M. Phosphonic Acid Anchored Tripodal Molecular Films on Indium Tin Oxide. *Phys. Chem. Chem. Phys.* **2024**, *26*, 11360–11369. [CrossRef] [PubMed]
83. Fournier, O.; Bapaume, C.D.; Messou, D.; Bouttemy, M.; Schulz, P.; Ozanam, F.; Lombez, L.; Schneider, N.; Rousset, J. Chemical Passivation with Phosphonic Acid Derivatives of ZnO Deposited by Atomic Layer Deposition and Its Influence on the Halide Perovskite Interface. *ACS Appl. Energy Mater.* **2021**, *4*, 5787–5797. [CrossRef]
84. Lange, I.; Reiter, S.; Pätzel, M.; Zykov, A.; Nefedov, A.; Hildebrandt, J.; Hecht, S.; Kowarik, S.; Wöll, C.; Heimel, G.; et al. Tuning the Work Function of Polar Zinc Oxide Surfaces Using Modified Phosphonic Acid Self-Assembled Monolayers. *Adv. Funct. Mater.* **2014**, *24*, 7014–7024. [CrossRef]
85. Wu, T.; Mariotti, S.; Ji, P.; Ono, L.K.; Guo, T.; Rabehi, I.N.; Yuan, S.; Zhang, J.; Ding, C.; Guo, Z.; et al. Self-Assembled Monolayer Hole-Selective Contact for Up-Scalable and Cost-Effective Inverted Perovskite Solar Cells. *Adv. Funct. Mater.* **2024**, *34*, 2316500. [CrossRef]
86. Song, D.; Narra, S.; Li, M.Y.; Lin, J.S.; Diau, E.W.G. Interfacial Engineering with a Hole-Selective Self-Assembled Monolayer for Tin Perovskite Solar Cells via a Two-Step Fabrication. *ACS Energy Lett.* **2021**, *6*, 4179–4186. [CrossRef]
87. Ullah, A.; Park, K.H.; Nguyen, H.D.; Siddique, Y.; Shah, S.F.A.; Tran, H.; Park, S.; Lee, S.I.; Lee, K.K.; Han, C.H.; et al. Novel Phenothiazine-Based Self-Assembled Monolayer as a Hole Selective Contact for Highly Efficient and Stable p-i-n Perovskite Solar Cells. *Adv. Energy Mater.* **2022**, *12*, 2103175. [CrossRef]
88. Xie, L.; Chen, J.; Vashishtha, P.; Zhao, X.; Shin, G.S.; Mhaisalkar, S.G.; Park, N.G. Importance of Functional Groups in Cross-Linking Methoxysilane Additives for High-Efficiency and Stable Perovskite Solar Cells. *ACS Energy Lett.* **2019**, *4*, 2192–2200. [CrossRef]
89. Guo, H.; Liu, C.; Hu, H.; Zhang, S.; Ji, X.; Cao, X.M.; Ning, Z.; Zhu, W.H.; Tian, H.; Wu, Y. Neglected Acidity Pitfall: Boric Acid-Anchoring Hole-Selective Contact for Perovskite Solar Cells. *Natl. Sci. Rev.* **2023**, *10*, nwad057. [CrossRef]
90. Cassella, E.J.; Spooner, E.L.K.; Thornber, T.; O'Kane, M.E.; Catley, T.E.; Bishop, J.E.; Smith, J.A.; Game, O.S.; Lidzey, D.G. Gas-Assisted Spray Coating of Perovskite Solar Cells Incorporating Sprayed Self-Assembled Monolayers. *Adv. Sci.* **2022**, *9*, 2104848. [CrossRef]
91. Zheng, X.; Li, Z.; Zhang, Y.; Chen, M.; Liu, T.; Xiao, C.; Gao, D.; Patel, J.B.; Kuciauskas, D.; Magomedov, A.; et al. Co-Deposition of Hole-Selective Contact and Absorber for Improving the Processability of Perovskite Solar Cells. *Nat. Energy* **2023**, *8*, 462–472. [CrossRef]
92. Zhan, L.; Zhang, S.; Li, Z.; Li, W.; Zhang, H.; He, J.; Ji, X.; Liu, S.; Yu, F.; Wang, S.; et al. Anchorable Polymers Enabling Ultra-Thin and Robust Hole-Transporting Layers for High-Efficiency Inverted Perovskite Solar Cells. *Angew. Chem.-Int. Ed.* **2025**, *64*, 202422571. [CrossRef]
93. Chen, T.P.; Lin, C.W.; Li, S.S.; Tsai, Y.H.; Wen, C.Y.; Lin, W.J.; Hsiao, F.M.; Chiu, Y.P.; Tsukagoshi, K.; Osada, M.; et al. Self-Assembly Atomic Stacking Transport Layer of 2D Layered Titania for Perovskite Solar Cells with Extended UV Stability. *Adv. Energy Mater.* **2018**, *8*, 1701722. [CrossRef]
94. Huang, Y.; Tao, M.; Zhang, Y.; Wang, Z.; Sun, Z.; Zhang, W.; Xiong, Y.; Zong, X.; Wang, Y.; Liang, M. Asymmetric Modification of Carbazole Based Self-Assembled Monolayers by Hybrid Strategy for Inverted Perovskite Solar Cells. *Angew. Chem.-Int. Ed.* **2024**, *64*, e202416188. [CrossRef]
95. Bi, H.; Liu, J.; Wang, L.; Liu, T.; Zhang, Z.; Shen, Q.; Hayase, S. Selective Contact Self-Assembled Molecules for High-Performance Perovskite Solar Cells. *eScience* **2025**, *5*, 100329. [CrossRef]
96. Pauls, A.; Dunnum, A.; Martin, A.; Huth, A.; Du, C.; Thuo, M. Correcting Edge Defects in Self-Assembled Monolayers through Thermal Annealing. *ChemPhysChem* **2024**, *25*, e202400626. [CrossRef] [PubMed]
97. Yang, G.; Wang, C.; Lei, H.; Zheng, X.; Qin, P.; Xiong, L.; Zhao, X.; Yan, Y.; Fang, G. Interface Engineering in Planar Perovskite Solar Cells: Energy Level Alignment, Perovskite Morphology Control and High Performance Achievement. *J. Mater. Chem. A* **2017**, *5*, 1658–1666. [CrossRef]
98. Lee, J.H.; Kim, B.S.; Park, J.; Lee, J.W.; Kim, K. Opportunities and Challenges for Perovskite Solar Cells Based on Vacuum Thermal Evaporation. *Adv. Mater. Technol.* **2023**, *8*, 2200928. [CrossRef]

99. Gaur, N.; Misra, M.; Hossain, K.; Kabra, D. Improved Thermally Activated Delayed Fluorescence-Based Electroluminescent Devices Using Vacuum-Processed Carbazole-Based Self-Assembled Monolayers. *ACS Energy Lett.* **2024**, *9*, 1056–1062. [CrossRef]
100. Du, P.; Wang, L.; Li, J.; Luo, J.; Ma, Y.; Tang, J.; Zhai, T. Thermal Evaporation for Halide Perovskite Optoelectronics: Fundamentals, Progress, and Outlook. *Adv. Opt. Mater.* **2022**, *10*, 2101770. [CrossRef]
101. Choi, Y.; Koo, D.; Jeong, M.; Jeong, G.; Lee, J.; Lee, B.; Choi, K.J.; Yang, C.; Park, H. Toward All-Vacuum-Processable Perovskite Solar Cells with High Efficiency, Stability, and Scalability Enabled by Fluorinated Spiro-OMeTAD through Thermal Evaporation. *Sol. RRL* **2021**, *5*, 2100415. [CrossRef]
102. Wang, Z.; Lyu, M.; Zhang, B.W.; Xiao, M.; Zhang, C.; Han, E.Q.; Wang, L. Thermally Evaporated Metal Halide Perovskites and Their Analogues: Film Fabrication, Applications and Beyond. *Small Methods* **2024**, *9*, e2301633. [CrossRef]
103. Bae, S.R.; Heo, D.Y.; Kim, S.Y. Recent Progress of Perovskite Devices Fabricated Using Thermal Evaporation Method: Perspective and Outlook. *Mater. Today Adv.* **2022**, *14*, 100232. [CrossRef]
104. Kosasih, F.U.; Erdenebileg, E.; Mathews, N.; Mhaisalkar, S.G.; Bruno, A. Thermal Evaporation and Hybrid Deposition of Perovskite Solar Cells and Mini-Modules. *Joule* **2022**, *6*, 2692–2734. [CrossRef]
105. Yuan, Q.; Lohmann, K.B.; Oliver, R.D.J.; Ramadan, A.J.; Yan, S.; Ball, J.M.; Christoforo, M.G.; Noel, N.K.; Snaith, H.J.; Herz, L.M.; et al. Thermally Stable Perovskite Solar Cells by All-Vacuum Deposition. *ACS Appl. Mater. Interfaces* **2023**, *15*, 772–781. [CrossRef]
106. Farag, A.; Feeney, T.; Hossain, I.M.; Schackmar, F.; Fassl, P.; Küster, K.; Bäuerle, R.; Ruiz-Preciado, M.A.; Hentschel, M.; Ritzer, D.B.; et al. Evaporated Self-Assembled Monolayer Hole Transport Layers: Lossless Interfaces in *p-i-n* Perovskite Solar Cells. *Adv. Energy Mater.* **2023**, *13*, 2203982. [CrossRef]
107. Chen, B.; Peng, C.; Guo, R.; He, Z.; Sun, L.; Zhang, F.; He, X.; Zeng, H.; Wang, L. Dual-Function Self-Assembled Molecules as Hole-Transport Layers for Thermally Evaporated High-Efficiency Blue Perovskite Light-Emitting Diodes. *Adv. Mater.* **2024**, *37*, e2411451. [CrossRef] [PubMed]
108. Kore, B.P.; Er-Raji, O.; Fischer, O.; Callies, A.; Schultz-Wittmann, O.; Schulze, P.S.C.; Bivour, M.; De Wolf, S.; Glunz, S.W.; Borchert, J. Efficient Fully Textured Perovskite Silicon Tandems with Thermally Evaporated Hole Transporting Materials. *Energy Environ. Sci.* **2024**, *18*, 354–366. [CrossRef]
109. Mariotti, S.; Rabehi, I.N.; Zhang, C.; Huo, X.; Zhang, J.; Ji, P.; Wu, T.; Li, T.; Yuan, S.; Liu, X.; et al. Unraveling the Morphological and Energetic Properties of 2PACz Self-Assembled Monolayers Fabricated With Upscaling Deposition Methods. *Energy Environ. Mater.* **2024**, *8*, e12825. [CrossRef]
110. Li, J.; Li, S.; He, B.; Zheng, R.; Wang, Y.; Chen, S. An Energy Level Alignment Study of 2PACz Molecule on Perovskite Device-Related Interfaces by Vacuum Deposition. *Adv. Energy Sustain. Res.* **2025**, 2400336. [CrossRef]
111. JIANG, W.; Wang, D.; Shang, W.; Li, Y.; Zeng, J.; Zhu, P.; Zhang, B.; Mei, L.; Chen, X.-K.; Xu, Z.-X.; et al. Spin-coated and Vacuum-processed Hole-extracting Self-assembled Multilayers with H-aggregation for High-performance Inverted Perovskite Solar Cells. *Angew. Chemie Int. Ed.* **2024**, *63*, e202411730. [CrossRef]
112. Zhang, S.; Jiang, X.; Wang, X.; Gao, Y.; Hou, T.A.; Teng, X.; Wang, H.; Chen, W.; Gao, S.; Li, X.; et al. Complementary Self-Assembled Monolayers Enabling Improved Energy Level Alignment in Inverted Perovskite Solar Cells. *J. Energy Chem.* **2025**, *104*, 136–145. [CrossRef]
113. Al-Ashouri, A.; Marčinskas, M.; Kasparavičius, E.; Malinauskas, T.; Palmstrom, A.; Getautis, V.; Albrecht, S.; McGehee, M.D.; Magomedov, A. Wettability Improvement of a Carbazole-Based Hole-Selective Monolayer for Reproducible Perovskite Solar Cells. *ACS Energy Lett.* **2023**, *8*, 898–900. [CrossRef]
114. Zhang, S.; Ye, F.; Wang, X.; Chen, R.; Zhang, H.; Zhan, L.; Jiang, X.; Li, Y.; Ji, X.; Liu, S.; et al. Minimizing Buried Interfacial Defects for Efficient Inverted Perovskite Solar Cells. *Science* **2023**, *380*, 404–409. [CrossRef]
115. Lee, S.H.; Lee, H.J.; Kim, D.H.; Noh, Y.J.; Kwon, S.N.; Kim, D.H.; Na, S.I. Vacuum-Assisted Deposition of Highly Hydrophobic Self-Assembled Monolayer for High-Efficiency Perovskite Solar Cells. *Sol. RRL* **2024**, *8*, 2400170. [CrossRef]
116. Li, T.; Wang, K.; Tong, Y.; Qi, H.; Yue, S.; Li, W.; Wang, H. In Situ Dehydration Condensation of Self-Assembled Molecules Enables Stabilization of CsPbI3 Perovskites for Efficient Photovoltaics. *Adv. Funct. Mater.* **2024**, *34*, 2409621. [CrossRef]
117. Wagstaffe, M.; Thomas, A.G.; Jackman, M.J.; Torres-Molina, M.; Syres, K.L.; Handrup, K. An Experimental Investigation of the Adsorption of a Phosphonic Acid on the Anatase TiO2(101) Surface. *J. Phys. Chem. C* **2016**, *120*, 1693–1700. [CrossRef]
118. Shao, S.; Loi, M.A. The Role of the Interfaces in Perovskite Solar Cells. *Adv. Mater. Interfaces* **2020**, *7*, 1901469.
119. Zhang, J.; Yang, J.; Dai, R.; Sheng, W.; Su, Y.; Zhong, Y.; Li, X.; Tan, L.; Chen, Y. Elimination of Interfacial Lattice Mismatch and Detrimental Reaction by Self-Assembled Layer Dual-Passivation for Efficient and Stable Inverted Perovskite Solar Cells. *Adv. Energy Mater.* **2022**, *12*, 2103674. [CrossRef]
120. Mann, D.S.; Patil, P.; Kwon, S.N.; Na, S.I. Enhanced Performance of P-i-n Perovskite Solar Cell via Defect Passivation of Nickel Oxide/Perovskite Interface with Self-Assembled Monolayer. *Appl. Surf. Sci.* **2021**, *560*, 149973. [CrossRef]
121. Isikgor, F.H.; Subbiah, A.S.; Eswaran, M.K.; Howells, C.T.; Babayigit, A.; De Bastiani, M.; Yengel, E.; Liu, J.; Furlan, F.; Harrison, G.T.; et al. Scaling-up Perovskite Solar Cells on Hydrophobic Surfaces. *Nano Energy* **2021**, *81*, 105633. [CrossRef]

122. Wang, Y.; Duan, L.; Zhang, M.; Hameiri, Z.; Liu, X.; Bai, Y.; Hao, X. PTAA as Efficient Hole Transport Materials in Perovskite Solar Cells: A Review. *Sol. RRL* **2022**, *6*, 2200234. [CrossRef]
123. Xu, J.; Dai, J.; Dong, H.; Li, P.; Chen, J.; Zhu, X.; Wang, Z.; Jiao, B.; Hou, X.; Li, J.; et al. Surface-Tension Release in PTAA-Based Inverted Perovskite Solar Cells. *Org. Electron.* **2022**, *100*, 106378. [CrossRef]
124. Kuan, C.H.; Luo, G.S.; Narra, S.; Maity, S.; Hiramatsu, H.; Tsai, Y.W.; Lin, J.M.; Hou, C.H.; Shyue, J.J.; Diau, E.W.-G. How Can a Hydrophobic Polymer PTAA Serve as a Hole- Transport Layer for an Inverted Tin Perovskite Solar Cell? *Chem. Eng. J.* **2022**, *450*, 138037. [CrossRef]
125. Scarfato, P.; Schiavone, N.; Rossi, G.; Incarnato, L. An Easy Route to Wettability Changes of Polyethylene Terephthalate-Silicon Oxide Substrate Films for High Barrier Applications, Surface-Modified with a Self-Assembled Monolayer of Fluoroalkylsilanes. *Polymers* **2019**, *11*, 257. [CrossRef] [PubMed]
126. Yılmaz, T. Improving the Performance Parameters of Organic Field-Effect Transistors via Alkyl Chain Length of Boronic Acid Self-Assembled Monolayers. *J. Mater. Sci. Mater. Electron.* **2024**, *35*, 966. [CrossRef]
127. Zhao, Y.; Luan, X.; Han, L.; Wang, Y. Post-Assembled Alkylphosphonic Acids for Efficient and Stable Inverted Perovskite Solar Cells. *Adv. Funct. Mater.* **2024**, *34*, 2405646. [CrossRef]
128. Pylnev, M.; Barbisan, A.M.; Wei, T.C. Effect of Wettability of Substrate on Metal Halide Perovskite Growth. *Appl. Surf. Sci.* **2021**, *541*, 148559. [CrossRef]
129. Li, E.; Bi, E.; Wu, Y.; Zhang, W.; Li, L.; Chen, H.; Han, L.; Tian, H.; Zhu, W.H. Synergistic Coassembly of Highly Wettable and Uniform Hole-Extraction Monolayers for Scaling-up Perovskite Solar Cells. *Adv. Funct. Mater.* **2020**, *30*, 1909509. [CrossRef]
130. Zhu, W.; Yang, M.; Han, T.; Wang, Y.; Luo, X.; Chai, W.; Xi, H.; Zhou, L.; Chen, D.; Zhang, J.; et al. Homogeneous Crystallization of MA-Free, Wide-Bandgap Perovskite Films via Self-Assembled Monolayer Capping for Laminated Silicon/Perovskite Tandem Solar Cells. *Chem. Eng. J.* **2024**, *500*, 156798. [CrossRef]
131. Wang, Z.; Duan, X.; Zhang, J.; Yuan, W.; Qu, D.; Chen, Y.; He, L.; Wang, H.; Yang, G.; Zhang, W.; et al. Manipulating the Crystallization Kinetics of Halide Perovskites for Large-Area Solar Modules. *Commun. Mater.* **2024**, *5*, 131. [CrossRef]
132. Ali, F.; Roldán-Carmona, C.; Sohail, M.; Nazeeruddin, M.K. Applications of Self-Assembled Monolayers for Perovskite Solar Cells Interface Engineering to Address Efficiency and Stability. *Adv. Energy Mater.* **2020**, *10*, 2002989. [CrossRef]
133. Li, M.; Sun, R.; Chang, J.; Dong, J.; Tian, Q.; Wang, H.; Li, Z.; Yang, P.; Shi, H.; Yang, C.; et al. Orientated Crystallization of FA-Based Perovskite via Hydrogen-Bonded Polymer Network for Efficient and Stable Solar Cells. *Nat. Commun.* **2023**, *14*, 573. [CrossRef] [PubMed]
134. Jiang, W.; Hu, Y.; Li, F.; Lin, F.R.; Jen, A.K.Y. Hole-Selective Contact with Molecularly Tailorable Reactivity for Passivating High-Performing Inverted Perovskite Solar Cells. *CCS Chem.* **2024**, *6*, 1654–1661. [CrossRef]
135. Chen, M.; Kapil, G.; Wang, L.; Sahamir, S.R.; Baranwal, A.K.; Nishimura, K.; Sanehira, Y.; Zhang, Z.; Kamarudin, M.A.; Shen, Q.; et al. High Performance Wide Bandgap Lead-Free Perovskite Solar Cells by Monolayer Engineering. *Chem. Eng. J.* **2022**, *436*, 135196. [CrossRef]
136. Zeng, J.; Bi, L.; Cheng, Y.; Xu, B.; Jen, A.K.Y. Self-Assembled Monolayer Enabling Improved Buried Interfaces in Blade-Coated Perovskite Solar Cells for High Efficiency and Stability. *Nano Res. Energy* **2022**, *1*, e9120004. [CrossRef]
137. Zuo, L.; Gu, Z.; Ye, T.; Fu, W.; Wu, G.; Li, H.; Chen, H. Enhanced Photovoltaic Performance of $CH_3NH_3PbI_3$ Perovskite Solar Cells through Interfacial Engineering Using Self-Assembling Monolayer. *J. Am. Chem. Soc.* **2015**, *137*, 2674–2679. [CrossRef]
138. Huang, Z.; Ge, X.; Liu, Z.; Shi, B.; Wang, P.; Zhao, Y.; Zhang, X. Highly Efficient Blade-Coated 1.67 EV p-i-n Perovskite Solar Cells Enabled by a Hybrid Self-Assembled Monolayer and Surface Passivation. *ACS Appl. Energy Mater.* **2024**, *7*, 11683–11690. [CrossRef]
139. Liu, M.; Li, M.; Li, Y.; An, Y.; Yao, Z.; Fan, B.; Qi, F.; Liu, K.; Yip, H.L.; Lin, F.R.; et al. Defect-Passivating and Stable Benzothiophene-Based Self-Assembled Monolayer for High-Performance Inverted Perovskite Solar Cells. *Adv. Energy Mater.* **2024**, *14*, 2303742. [CrossRef]
140. Jiang, W.; Liu, M.; Li, Y.; Lin, F.R.; Jen, A.K.Y. Rational Molecular Design of Multifunctional Self-Assembled Monolayers for Efficient Hole Selection and Buried Interface Passivation in Inverted Perovskite Solar Cells. *Chem. Sci.* **2024**, *15*, 2778–2785. [CrossRef]
141. Alghamdi, A.R.M.; Yanagida, M.; Shirai, Y.; Andersson, G.G.; Miyano, K. Surface Passivation of Sputtered NiO_x Using a SAM Interface Layer to Enhance the Performance of Perovskite Solar Cells. *ACS Omega* **2022**, *7*, 12147–12157. [CrossRef]
142. Ball, J.M.; Petrozza, A. Defects in Perovskite-Halides and Their Effects in Solar Cells. *Nat. Energy* **2016**, *1*, 16149. [CrossRef]
143. Meggiolaro, D.; Mosconi, E.; De Angelis, F. Formation of Surface Defects Dominates Ion Migration in Lead-Halide Perovskites. *ACS Energy Lett.* **2019**, *4*, 779–785. [CrossRef]
144. Naguib, A.; Elseman, A.M.; Ishak, E.A.; El-Gaby, M.S.A. Novel Hole Transport Materials of Pyrogallol-Sulfonamide Hybrid: Synthesis, Optical, Electrochemical Properties and Molecular Modelling for Perovskite Solar Cells. *Mater. Renew. Sustain. Energy* **2025**, *14*, 3. [CrossRef]

145. Fadl, A.M.M.; Elseman, A.M.; El-Adasy, A.B.A.A.M.; Rashad, M.M.; El-Gaby, M.S.A. Passivator Materials Based on the Benzothiazole-Sulfonamide Hybrid: Synthesis, Optical, Electrochemical Properties, and Molecular Modeling for Perovskite Solar Cells. *Mater. Res. Bull.* **2025**, *182*, 113151. [CrossRef]
146. Cassella, E.J.; Spooner, E.L.K.; Smith, J.A.; Thornber, T.; O'Kane, M.E.; Oliver, R.D.J.; Catley, T.E.; Choudhary, S.; Wood, C.J.; Hammond, D.B.; et al. Binary Solvent System Used to Fabricate Fully Annealing-Free Perovskite Solar Cells. *Adv. Energy Mater.* **2023**, *13*, 2203468. [CrossRef]
147. Zhu, T.; Su, J.; Labat, F.; Ciofini, I.; Pauporté, T. Interfacial Engineering through Chloride-Functionalized Self-Assembled Monolayers for High-Performance Perovskite Solar Cells. *ACS Appl. Mater. Interfaces* **2020**, *12*, 744–752. [CrossRef]
148. Tan, Q.; Li, Z.; Luo, G.; Zhang, X.; Che, B.; Chen, G.; Gao, H.; He, D.; Ma, G.; Wang, J.; et al. Inverted Perovskite Solar Cells Using Dimethylacridine-Based Dopants. *Nature* **2023**, *620*, 545–551. [CrossRef]

Disclaimer/Publisher's Note: The statements, opinions and data contained in all publications are solely those of the individual author(s) and contributor(s) and not of MDPI and/or the editor(s). MDPI and/or the editor(s) disclaim responsibility for any injury to people or property resulting from any ideas, methods, instructions or products referred to in the content.